Modelling Biofilm Activity in Bioretention Cells

by

Tao Yu

A Thesis Submitted in Partial Fulfillment
of the Requirements for the Degree of

MASTER OF APPLIED SCIENCE

in the Department of Mechanical Engineering

Supervisory Committee

Modelling Biofilm Activity in Bioretention Cells

by

Tao Yu

Supervisory Committee

Dr. Caterina Valeo, Supervisor
(Department of Mechanical Engineering)

Dr. Phalguni Mukhopadhyaya, Member
(Department of Mechanical Engineering)

Abstract

Supervisory Committee

Dr. Caterina Valeo, Supervisor
(Department of Mechanical Engineering)

Dr. Phalguni Mukhopadhyaya, Member
(Department of Mechanical Engineering)

Biofilms can be simply defined as communities of microbes attached to a surface. There are various types of biofilm, which can be either beneficial or harmful to an ecosystem. Good biofilm offers valuable services to society or in the function of natural ecosystems such as those that contribute to controlled bioremediation of ground water and soils in Low Impact Development approaches called bioretention cell. This thesis researched ways to model biofilm activity at the field-scale and used experimental data (BOD_5 and NO_3^-) to verify these models. Two mathematical models are presented in this work. The first model provides and tests the solution of substrate and biomass concentration while the second model modified the expression for the substrate flux into the biofilm. They are analyzed using a sensitivity analysis and their performance is compared using field-scale data. The solution for concentration is computed with some selected values of dimensionless biofilm thickness (0.0375 and 3.75) and dimensionless substrate concentration outside of the biofilm (0.005 to 0.5), which shows these two variables significantly affect model results. The simulations illustrate that biofilm activity mostly occurs in the summer while the substrate flux is normally stable at similar levels in the same season.

Table of Contents

List of Tables

List of Figures

Notation

Symbols

a	specific surface area (m^{-1})
b_{det}	first-order biomass detachment loss rate per day
b	microbial death constant
b'	total first-order biofilm mass decay and detachment coefficient
b_t	first order decay and shear loss rates
C_O	Bulk liquid concentration of oxygen
D_f	substrate's diffusion coefficient in the biofilm (m^2/day)
D_l	diffusion coefficient in the liquid phase
D_w	molecular diffusion coefficient in water
f	ratio between flux into actual and deep biofilm
J	substrate flux into biofilm ($mg*cm^{-2}d^{-1}$)
J^*	dimensionless substrate flux
J_{deep}^*	dimensionless substrate flux into deep biofilm
K	Michaelis-Menten constant
Km	maximum specific rate of substrate utilization
K_d	specific decay rate,
K_s	Monod half-velocity coefficient
K_O	Oxygen half saturation constant of microorganism
K_1	substrate's first-order utilization coefficient (day^{-1})
k_{det}	detachment rate constant
L_l	boundary layer thickness (cm)
L_f^*	dimensionless biofilm thickness
L_f	biofilm thickness (cm)
L_i	substrate concentration from the inlet (ultimate BOD, mg/cm^3)
L_o	substrate concentration from the outlet (ultimate BOD, mg/cm^3)
q_{max}^s	maximum specific substrate uptake rate of the microorganism
q	substrate consumption rate constant
Q	volumetric flow rate m^3/day
r_x	biomass growth rate
r_o	oxygen consumption rate
r_{det}	detachment rate
S_b	substrate concentration in the bulk liquid (mg/cm^3)
Ss	substrate concentration at the biofilm layer interface (mg/cm^3)
S_1	substrate concentration outside the biofilm (mg/cm^3)
S	substrate concentration in the system's effluent
S_L	dimensionless substrate concentration outside the biofilm
S_f	substrate concentration in the biofilm (mg/cm^3)
S^*	dimensionless effluent substrate concentration
S^*_{min}	dimensionless minimum substrate concentration that can sustain biofilm
S^*_s	dimensionless minimum substrate concentration at the diffusion layer
S_{min}	minimum substrate concentration that can sustain biofilm
Si	substrate concentration from the inlet (Nitrate) (mg/cm^3)

So	substrate concentration from the outlet (Nitrate) (mg/cm^3)
S_{bo}	dimensionless substrate concentration within biofilm
S^o	influent substrate concentration (mg/cm^3)
S_{bo}	bulk liquid concentration of oxygen (mg/cm^3)
t	time
V	system volume m^3
x	dimensionless co-ordinate
X	distance to the solid surface
X_f	biomass concentration with the biofilm (mg/cm^3)
Y	yield coefficient
z	co-ordinate
z^*	dimensionless distance normal to the biofilm thickness
Z	direction along the biofilm thickness
α	product coefficient
β	exponential coefficient
δ	dimensionless biofilm thickness
ψ	dimensionless concentration flux into the biofilm
Fe^{2+}	ferrous iron
NH_3	ammonia
NH^{4+}	ammonium nitrogen
NO_3^-	nitrate
O_2	oxygen

Abbreviations

BOD	biochemical oxygen demand
BOD_u	ultimate biochemical oxygen demand
BOD_5	five day biochemical oxygen demand
BDOC	biodegradable dissolved organic carbon
COD	chemical oxygen demand
EPS	extracellular polymeric substances
F	fall
HRT	hydraulic retention time
LID	low impact development
PGPR	plant growth-promoting rhizobacteria
S	summer
SRT	solids retention time
Sp	spring
TN	total nitrogen
TSS	total Suspended Solids
W	winter

Acknowledgments

I gratefully acknowledge the support from many people during the course of this work at the University of Victoria. Professor Caterina Valeo, my supervisor, has provided not only her wealth of knowledge and research experiences in all aspects, but also continuous encouragement and financial support.

I would also like to thank my great friend on campus, Usman, for his kindly help on my thesis and continuous encouragement during this period.

Finally, I really want to thank both my wonderful wife, Jie Zhong, and my lovely parents. Thank you for supporting me for these past two years, I love you all.

Chapter 1: Introduction

1.1 Stormwater Pollution

In urban areas, there has been a growing concern that rainwater flowing onto impervious surfaces may accumulate a wide variety of contaminants, including nutrients, suspended sediments, heavy metals, hydrocarbons and organic chemicals (Pierre-Yves et al., 2014) that can adversely affect urban water quality and the ecological health of the receiving water bodies. Consideration for the effects of urban runoff on freshwater ecosystems has led to the implementation of Low Impact Development (LID) strategies (Barbosa et al., 2012; Pierre-Yves et al., 2014) including installation of retention ponds, wetlands, green roofs, bioretention cells (rain gardens), grassed swales, infiltration trenches and sand filters.

LID (Low Impact Development) is a term used in Canada and the United States, and is an approach to land production that works with nature to treat stormwater as close to its source as possible. The principles of LID focus on preserving and recreating natural landscape features, and minimizing effective imperviousness to create functional site drainage systems that manage stormwater as a resource rather than a waste product.

Bioretention is one promising type of LID. Bioretention is the process that contaminants and sediment are removed from stormwater runoff through physically retaining the polluted stormwater and allowing it to undergo biological, physical and chemical reactions leading to pollutant reduction (Khan, 2011). Bioretention cells consist of suitable plants, a mulch layer, and a highly permeable soil generally overlaying a sand and gravel layer (see Figure 1-1). Various pollutants are captured through a series of physical, chemical and biological processes as the ponded water flow into the soil media,

and pollutant removal and capture takes place on the surface and throughout the media. The removal processes, include infiltration, filtration, sedimentation and others occurring below the surface. The runoff drains to the bottom of the media, where it can percolate into the surrounding sub-soil or be discharged through an outlet pipe.

Vegetation is a very important element of a bioretention cell, and it is used to slow incoming stormwater, and allow for the attenuation of both the peak discharge and time of concentration of the incoming flow. Generally, it can consist of native vegetation, and depending on the size of the cell, they can range from small plants to large plants. The first main purpose of the plants is to provide a protective cover for the growing media. Also, plants provide the potential to remove contaminants from urban runoff, particularly through nutrient absorption. Moreover, plant roots can actively adsorb pollutants from the water, and root growth and biological activity can promote infiltration and hydraulic conductivity. Therefore, a bioretention cell that is without plants can actually be a source of various pollutants.

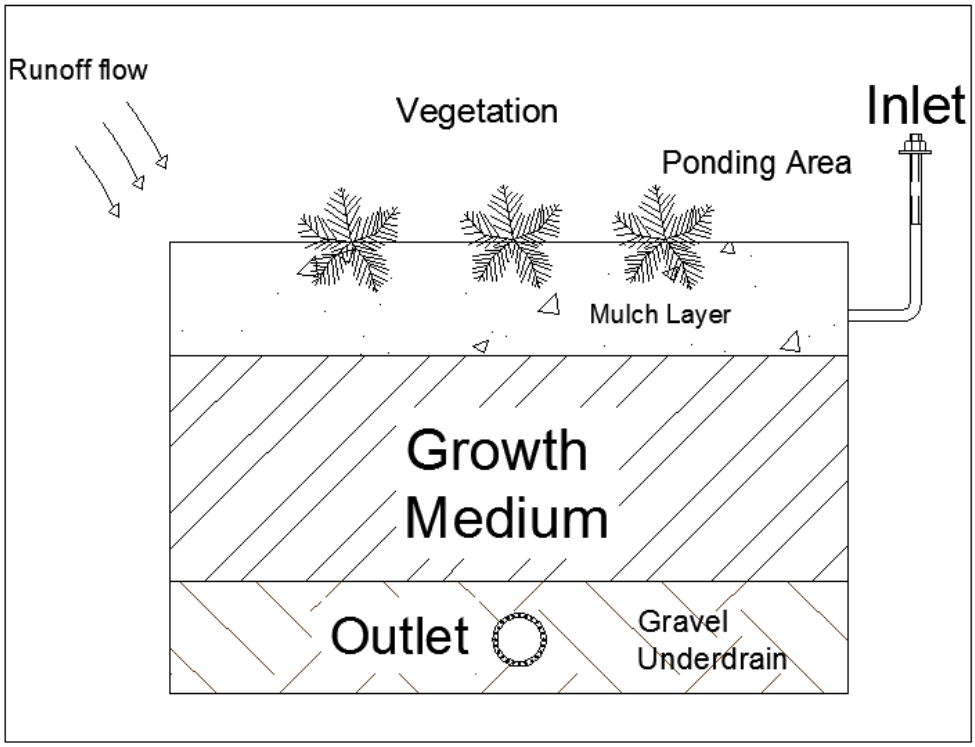

Figure 1- 1: a) The Layout for a typical Bioretention Cell; b) A small test cell in Parking lot 6 at UVic

1.2 Bioretention for Stormwater Quality Treatment

Stormwater quality guidelines involve restrictions on the amount of specific contaminants prevalent in stormwater. These guidelines vary by region but generally speaking include Total Suspended Solids (TSS), nutrients (nitrogen and phosphorus compounds), organic material, heavy metals, hydro-carbons and bacteria (Khan, 2011).

The biological process is a very important process in bioretention cells because it is directly responsible for removing for nitrogen compounds and organics. Thus, nitrogen reduction in bioretention cells has been studied in previous studies both in the lab-scale and in the macro-scale (or field scale). Nitrogen can occur in various forms such as total nitrogen (TN), nitrate and nitrite and ammonia.

The mechanisms of nitrogen removal in bioretention cells are through nitrification and denitrification. For instance, Ammonia can be converted to nitrate under aerobic conditions, and then nitrate and nitrite are converted to nitrogen gas under that condition (Khan, 2011). Most bioretention cells should have adequate conditions to undergo nitrification. However, some issues include low influent concentrations, which lead to the differences being too slight to see any significant reduction. Significant reductions will only be observed when influent concentrations are sufficiently high (Khan, 2011).

Generally, bioretention cells are not very effective in reducing the concentration of nitrate because this requires anoxic conditions, which are often unattainable or at least inconsistent over time. Another potential issue with nitrogen removal is that in between rain events, continuous biological activity will turn nitrogen compounds into nitrate, and this nitrate will then be flushed from the system at the onset of the next event. This can increase nitrate concentrations with time. However, decomposing matter from the vegetation can cause similar effects. An improvement of nitrogen uptake with time is

noted by further research, and it is also indicated that vegetation may be the most important component for nitrogen removal in bioretention cells (Khan, 2011).

1.3 The Role of Biofilm in Bioretention Cells

There are two forms of bacterial growth: the first form being single cells (planktonic) and the other involves *sessile aggregates*; that is, bacteria are attached to surfaces and aggregate in a hydrated polymeric matrix of their own synthesis to form biofilms. The second form is commonly referred to as the biofilm mode of growth. The earliest studies of biofilms were observations of environmental microbes adhering to a wide range of surfaces, which included everything from river rocks to medical devices to hulls of ships (O'Toole et al., 2004). This definition has been expanded to include surfaces as far ranging as steel pipes, soils, medical implants, and epithelial cells. A definition that once generally applied to a solid-liquid interface has grown to include the air-water interface, or no obvious interface at all, as in bacterial aggregates in suspension. However, it is unknown what extent biofilms at these different interfaces share metabolic or physiological traits.

Biofilms that grow on and around plant tissues have begun to reveal their importance in plant-microbe interactions by a number of studies (Lear et al., 2012). Microbial ecologists and engineers used a variety of approaches to examine adhered bacteria and model their behavior. The physical properties of the surfaces to which bacteria adhere include roughness, hydrophobicity and hydrophilicity, and thus, conditioning films was an early important focus of study in the field, and they defined the experimental approaches utilized. As electron microscopic techniques advanced and were applied, a picture of microbial biofilms and their structure began to emerge. The field was

revolutionized by using confocal scanning laser microscopy, coupled with fluorescent markers, which allowed visualization of the live, hydrated biofilm (O'Toole et al., 2004). The confocal scanning laser microscopy studies gave us the first three-dimensional view of an undisturbed biofilm, and this methodology is still applied in current biofilm research (Costerton et al., 1995).

However, much work remains to be done, that include further research into the processes that drive the interaction between biofilm forming microbes and plants. Defined model systems focusing on a few select plant and bacterial species have been, and will continue to be, important to understanding the interactions mediated by biofilm forming microbes on plants.

1.4 Fundamental Characteristics of Biofilm Systems in Pollutant Treatment

In the water industry, there are seven fundamental characteristics for any biofilm system that control what microorganisms are present, the biofilm's physical properties, and how it affects water quality. In addition, each of them has a distinct role in defining the biofilm system and give valuable insight into why biofilms are beneficial or not (Rittmann, 2004).

The first fundamental characteristic of a biofilm system in the water industry is that the microorganisms in the biofilm gain energy for growth and maintenance by consuming something that we regard as a water pollutant (Rittmann, 2004). Generally, most pollutants are reduced compounds, or electron-donor substrates which involve organic materials and are represented by biochemical oxygen demand (BOD) or biodegradable dissolved organic carbon (BDOC), ammonium nitrogen (NH_4^+-N), or ferrous iron (Fe^{2+}). When the pollutant is a donor, the biofilm grows and sustains itself only when a suitable

acceptor is present in an adequate amount. When the goal is treatment, we normally supply the acceptor, often dissolved oxygen, by some engineering means, and the process must be designed to allow rapid and cost-effective acceptor supply (Rittmann, 2004). On the other hand, when the pollutant is an acceptor, we must provide the donor to ensure its full reduction and removal of the pollutant. If we want to minimize biofilm fouling when an acceptor a donor pollutant is present, the best way is to keep the other reactant out of the system.

The second characteristic of a biofilm system is the attachment surface or substratum. The substratum is named as the solid surface that provides the biofilm growth. There are three substratum features, the first one is the wide variety of surface types: rock, concrete, plastic, steel, wood and so on. These are the materials of biofilm carriers in treatment processes, pipes, heat exchangers, and other process equipment that comes into contact with water. The second feature is interactions between the substratum and the microorganisms in the biofilm are passive, relating to the texture or chemical reactivity of the substratum. The last feature is the substratum's specific surface area, or the substratum surface area divided by the system's volume. The specific surface area is given the symbol *a* and has units of m^{-1}, which arises from a reduction of units in m^2/m^3. In general, the specific surface area is inversely proportional to the size of the biofilm carrier (Rittmann, 2004). A very high value, *a* associated with sand-sized carriers, is larger than 1,000 m^{-1}. On the other hand, a low specific surface area is lower than 10 m^{-1}. A high specific surface area means that reactions in the biofilm have a high potential to affect concentrations of substrates in the water.

The third characteristic is the physical structure of the biofilm. Some biofilms are

densely packed with biomass often referred to as biomass density (X_f, in mg/cm^3) approaching the maximum packing density of about 200 to 300 mg dry weight per cm^3. Other biofilms have an open structure composed of biomass clusters surrounded by water-filled channels, with an average X_f of only a few percent of the maximum density possible (Rittmann, 2004).

The fourth characteristic is that the biofilm residence time in the system normally is much larger than the residence time of the water. In addition, there are two different retention times. The average residence time for the water is the hydraulic retention time (*HRT*):

$$HRT = \frac{V}{Q} \qquad (1)$$

in which V is system volume (m^3), Q is volumetric flow rate (m^3/day), and *HRT* is in days. The other one is the average residence time for the biofilm biomass is the solids retention time (*SRT*), defined as (Rittmann, 2004):

$$SRT = \frac{active\ biomass\ in\ kg}{rate\ of\ active\ biomass\ detachment, in\ \frac{kg}{day}} = \frac{1}{b_{det}} \quad (2)$$

in which b_{det} is the first-order biomass detachment loss rate per day and *SRT* is in days. Moreover, *SRT* is independent of *HRT*, which means the time that the water spends in the system is very different from the time that the biofilm spends in the system. On the other hand, *SRT* is much larger than the *HRT* in most practical situations. There are some cases that b_{det} approaches zero, making the *SRT* nearly infinite. So it is a great advantage for biofilm treatment technology when *SRT* is considerably larger than *HRT*, because the size of the process and its capital cost is greatly reduced. This cost advantage is quantified simply later in the sixth characteristic of biofilm systems.

Having *SRT* >> *HRT* is that the biomass per unit volume is much higher in the biofilm system than for a *chemostat* having the same *SRT*. The chemostat is a laboratory apparatus used for the continuous culture of microorganisms. Mathematically, this concentration advantage is given by solids concentration ratio *SRT/HRT* (Rittmann, 2004), which says that the biomass concentration in the biofilm system is *SRT/HRT* times larger than the concentration in a *chemostat* having the same *SRT* = *HRT*, as well as the same substrate removal. Therefore, the selective retention of biomass through its attachment to the substratum makes it possible to accumulate more biomass per unit volume, which results in having a smaller volume. In one word, all of this depends on having a relatively low value of b_{det}. In the water industry, biofilm systems often operate under more or less stable conditions for months, years, or even decades. Therefore, the biofilm often approaches a steady-state condition in which changes to the biofilm's physical structure and metabolic function are relatively small and occur gradually.

Concentration gradient is the fifth characteristic of biofilm systems, and it arise when the density of active biomass in the biofilm is high, creating a strong potential to consume substrate. There are three different kinds of substrate concentration gradients inside a biofilm: deep, shallow and fully penetrated. For a deep profile, the substrate concentration is driven to zero inside the biofilm. If the reaction potential or biofilm thickness is less, then a shallow gradient is possible. Finally, for biofilms that are very thin or have very slow substrate removal kinetics, the substrate concentration stays nearly the same throughout the biofilm, or the substrate fully penetrates the biofilm. It is possible to know whether a biofilm is deep, shallow, or fully penetrated by computing a

dimensionless biofilm thickness, L_f^* (Rittmann, 2004). For the simple case in which substrate is consumed according to kinetic values that are first order in substrate concentration (S_f) and biomass density (X_f),

$$L_f^* = L_f\left(\frac{k_1 X_f}{D_f}\right)^{0.5} \qquad (3)$$

in which k_1 = the substrate's first-order utilization coefficient (day^{-1}), X_f = the density of the biomass consuming the substrate (mg/cm^3), D_f = the substrate's diffusion coefficient in the biofilm (m^2/day), and L_f = the physical thickness of the biofilm (m). A biofilm is deep if L_f^* > about 10, while it is fully penetrated for values smaller than about 0.1 (Rittmann, 2004). The biofilm is shallow for the substrate when L_f^* is between these ranges, with the gradient increasing for larger L_f^*.

The substrate flux is another characteristic of the biofilm system. Substrate is utilized inside the biofilm and have to be transported from the bulk liquid, across the biofilm's outer surface, and then inside the biofilm. The transport is driven by the concentration gradient, which is totally or largely perpendicular to the biofilm's surface (Rittmann, 2004). Therefore, the critical rates are surface-reaction rates or fluxes. The substrate flux is given the symbol J and has units of $mg/cm^2.day$. When the system is at steady state, the substrate flux into the biofilm equals the flux out of the bulk liquid:

$$J = \frac{Q(S^o - S)}{aV} \qquad (4)$$

in which S^o = the substrate concentration in the system's influent mg/cm^3, and S = the substrate concentration in the system's effluent mg/cm^3. In addition, $Q(S^o\text{-}S)$ is the mg/day removal rate of substrate, which aV is the biofilm area (m^2). A desired substrate concentration in the liquid, S, is associated with a particular flux, J. When the flow rate,

Q, and the substrate concentration in the influent, S^o, are known, then Equation 4 can be rearranged to compute the necessary surface area of biofilm, aV in m^2:

$$aV = \frac{Q(S^o - S)}{J} \qquad (5)$$

We assume the biofilm system has a very large specific surface area, so a small V can provide the needed aV. On the other hand, a very large V is needed when a is small. This breakdown of how a and V individually affect aV, shows why a large specific surface area is so valuable for reducing capital costs. Volumetric loading (i.e., $Q(S^o-S)/V$, in $mg/cm^3 \cdot day$) provides valuable information about a biofilm process, moreover, volumetric loading is the dividend of two fundamental descriptors, J/a; J and a are the parameters that characterize the biofilm system for design or analysis (Rittmann, 2004).

There is another equation associated with the substrate flux J, which determines the amount of biomass that accumulates on the substratum. For active bacteria utilizing substrate at flux J:

$$X_f L_f = \frac{YJ}{b_{det} + b} \qquad (6)$$

in which $X_f L_f$ = the accumulation of the active biomass per unit surface area (mg/cm^2), Y = yield coefficient ($mg/mg_{)}$, and b = microbial death constant (per day). Depending on our goals, we may want to maintain a large or a small $X_f L_f$, and equation 6 indicates how we can have an effect on the biofilm accumulation. A large biofilm accumulation requires a large JY and a small $(b_{det}+b)$. On the other hand, $X_f L_f$ can be kept very small if Y or J is very small or $(b_{det}+b)$ is very large (Rittmann, 2004).

The final fundamental characteristic is that a biofilm has a relatively fixed architecture. In other words, the different types of active biomass, along with inert cells, EPS

(extracellular polymeric substances) promotes the attachment of other microorganisms, and mineral solids establish themselves in their most favorable locations or niches (Donlan, 2002). Because detachment acts most strongly at the outer surface of the biofilm, only the fastest growing types of biomass find this location favorable. Biofilm creates and maintains a relatively stable niche as a natural outcome of several of the other fundamental characteristics. Summarizing the ways in which they naturally establish a relatively stable architecture it is noted that (Rittmann, 2004):

i. Having several donor and acceptor substrates makes it possible to have different types of active biomass together in the same biofilm.
ii. Substrate-concentration gradients inside the biofilm create niches based on the ability to consume a particular substrate.
iii. Detachment at the outer surface creates niches based on the relative need for a species to be protected from detachment loss.
iv. A long *SRT* means that a large biofilm accumulation is possible, giving the biofilm significant physical thickness to accentuate concentration gradients and protected areas.
v. Long-term operation under stable conditions allows the biofilm to approach a steady-state condition.
vi. EPS more or less glues the different microbial types (including the inert biomass) into fixed relative positions.

On the other hand, an abrupt change to the conditions controlling the niches can bring about a sharp shift in the architecture of a biofilm. Examples of abrupt changes encountered in the water industry include (a) a sudden increase in substrate loading,

which causes rapid growth of active bacteria and increases $X_f L_f$, and (b) application of a disinfectant or a cleaning operation, which drastically increase $(b_{det}+b)$ and decreases $X_f L_f$.

1.5 Biofilm Formation in Vegetated Systems

Plenty of bacteria and fungi are able to colonize and form biofilms on plant surfaces (Ramey et al., 2004). The rhizosphere is the area that encloses the zone of soil around a plant root in which the plant root exerts an influence on the growth and distribution of microorganisms (Fuqua et al., 2001). Moreover, soil which is not part of the rhizosphere is referred to as bulk soil. It is the soil outside of the rhizosphere and is not penetrated by plant roots. Therefore, the concentration of the natural organic compounds is much lower in bulk soil than that of rhizosphere. Rhizoplane refers to the vegetative surface that biofilms adhere to. Rhizosphere contains both vegetation and soil but the rhizoplane contains only that part related to the vegetation.

The rhizosphere is a heterogeneous microenvironment which includes both biotic and abiotic factors (O'Toole et al., 2000). In order to form efficiently, rhizobacterial biofilm formers should firstly be able to attach to the root surface and then survive in the rhizosphere (Beattie, 2006). Secondly, it should make use of nutrients exuded by the plant root, and proliferate and form microcolonies. Finally, it should efficiently colonize the entire root system, and compete with indigenous microorganisms. Some researchers describe the rhizosphere as the area around a plant root that is inhabited by a unique population of microorganisms influenced by the chemicals released from plant roots (Compant et al., 2010). Due to the complexity and diversity of plants and their root systems, it is hard to define the size or shape of rhizosphere. However, it could be defined

according to the chemical, biological and physical properties for different plants which change vertically and horizontally in the soil itself. It will be in direct correlation to the physical structure of the root system and its secretions. Roots can secrete many different compounds, which can provide a number of functions needed to keep the rhizosphere balanced.

A selective group of rhizobacteria not only benefits from the nutrients secreted by the plant root but also beneficially influences the plant in a direct or indirect way, resulting in a stimulation of its growth. Plant growth-promoting rhizobacteria (PGPR) is defined as a group of microorganisms in the rhizosphere that promote plant growth by increasing nutrient availability and these plant growth-promoting rhizobacteria (PGPR) can be classified by their beneficial effects (Ghodsalavi et al., 2013).

1.5.1 The process of biofilm formation on the root surface

Given the concept of rhizobacteria and rhizosphere, biofilm form on the root surface and steps for biofilm formation are the next concern. Based on microscopic analyses, the entire process of biofilm formation can be described as three main sequential steps. First of all, biofilm development begins within initial attachment of planktonic cells to a surface. After that, the biofilm develops a complex three-dimensional structure through cell division and recruitment of additional planktonic cells. This stage typically represents the mature biofilm structure. Finally, under certain circumstances the biofilm can be detached or reorganized.

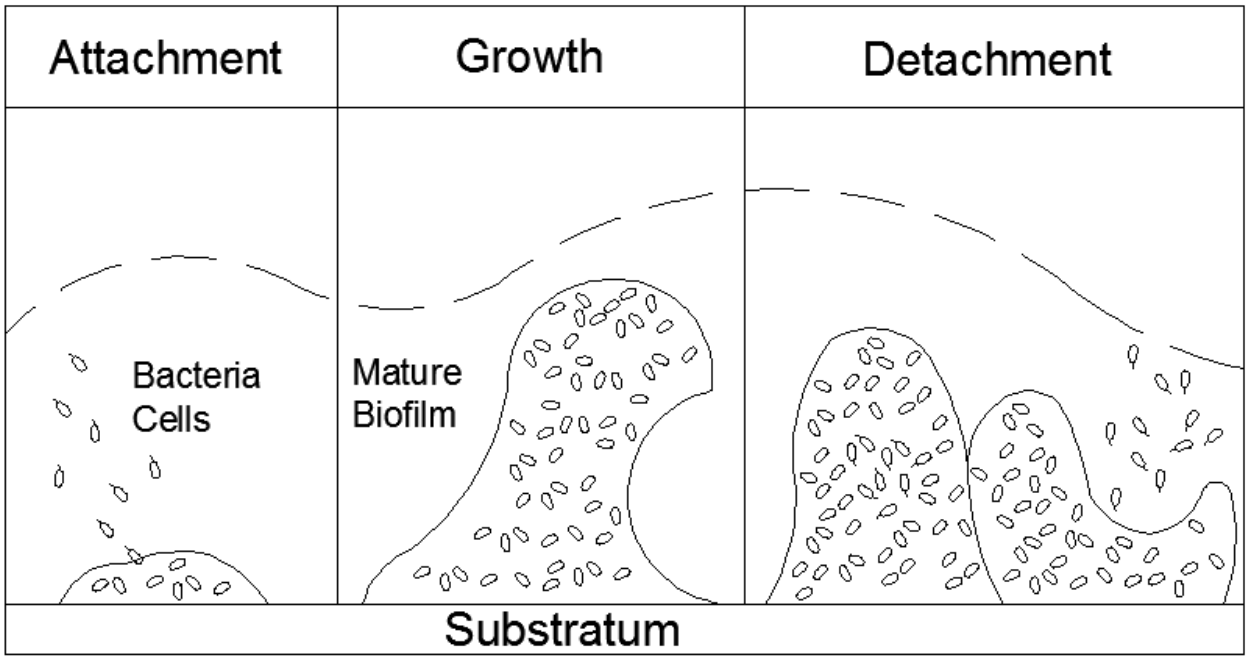

Figure 1- 2: Three main stages of biofilm formation (Modified from Peg Dirckx, 2003)

Figure 1-2 shows the biofilm life cycle illustrated in three steps: initial attachment events; the growth of complex biofilms; and detachment events by clumps of bacteria or by a 'swarming' phenomenon within the interior of bacterial clusters resulting in so-called 'seeding dispersal' (Stoodley and Dirckx, 2003).

Initial biofilm cell attachment occurs via physicochemical interactions and protein adhesion-secretion to form a cell monolayer (Prpich et al., 2006). Biofilm thickness is influenced by shear stress, nutrient availability and occurrence of toxic chemicals (Pastorella et al., 2012) with shear stress being the least important. The morphology of the solid phase or attaching surface can affect the biofilm. For instance, in sandy or fine particle soils, where shear stress is very low, biofilms on rock surfaces grow thinner because of the higher shear stress and lower specific area of the support (Pastorella et al., 2012). Detachment could be caused by changes in nutrient availability or hydrodynamic conditions, and it leads biofilm to spread along the groundwater flow. Detachment is also

related to bioremediation processes that involve engineered surfaces, such as biobarriers (Pastorella et al., 2012).

According to root secretions and cell debris formation, it is noted that the root tip is employed in maximum carbon turnover, because of the frequent ‘decapping’ of the root cap (Hawes et al., 2000). It could be predicted that differential bacterial biofilm formation would be least expected at the root tip level compared with the mature root regions. The biofilm depth in the root tip is less than in mature root regions; this variation may be due to fluctuations in the composition of the root exudates and nutrient availability at the root plane or specific secretion of antimicrobials from the root tip (Rudrappa et al., 2008). In addition, lateral roots in secretion and subsequent chemoattraction of bacteria leading to microcolony formation that may be the reason for increased biofilm thickness in mature regions of the root (Rudrappa et al., 2008). It is not known whether specific organic compounds secreted by roots also influence biofilm structures; thus, it is required to characterize these compounds from root exudates in the future study, and to know if those organic compounds inhibit rhizosphere biofilm formation or not.

1.5.2 Root Structure Definitions

In most vascular plants, roots are an underground structure that anchor the plant and absorb water and nutrients. New root tips grow continuously throughout the life of the plant and provide the surfaces through which most of the nutrients and water move. The major functions of roots, thus, can be summarized simply as absorption, conduction, storage, and anchorage.

There are four main regions of the root, and starting at the tip and moving upwards towards the stem are: root cap, zone of active cell division, zone of cell elongation and zone

of maturation (see Figure 1-3).

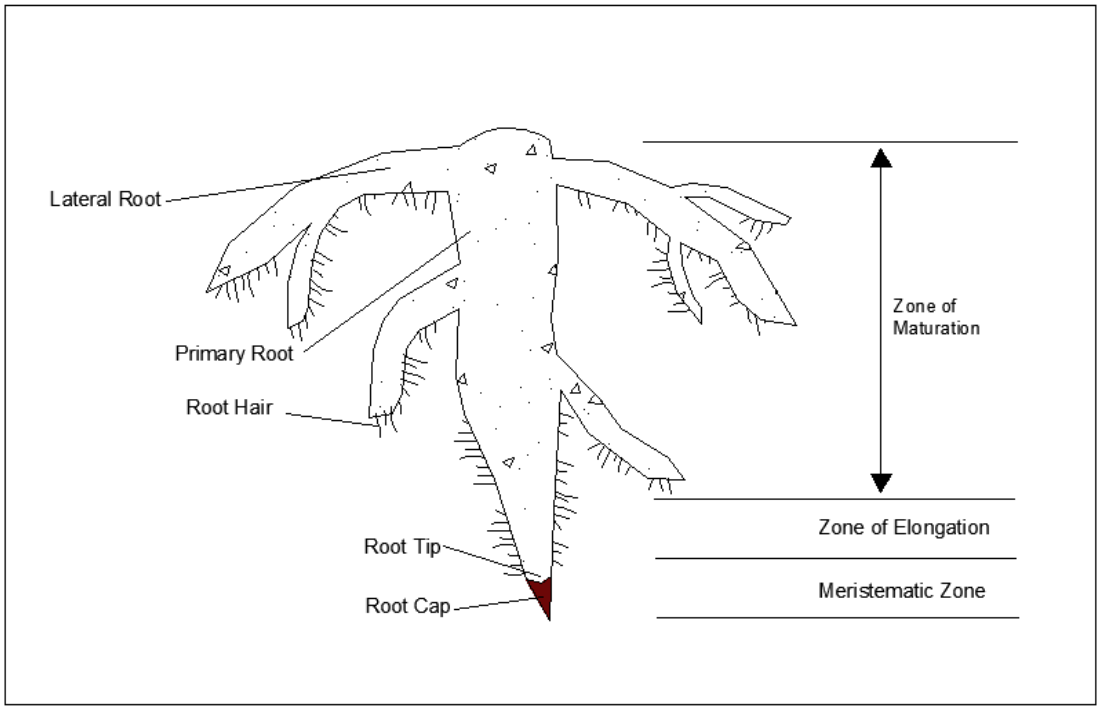

Figure 1- 3: External feature of a root

Zone of Maturation, is the pipeline section of the roots, conducting water and nutrients from the root hairs up to the stems. Zone of Elongation is the area where new cells are enlarging. The Root Tip is the region of cell division that supports root elongation, located at the root tips just behind the root cap. Root Cap is a thimble-shaped group of thick-walled cells at the root tip and serves to go through soil. The Root Cap protects the tender meristem tissues. Root Hairs are tubular extensions of epidermal cells of a root, serving to absorb water and mineral from soil. Root Hairs are extremely subject to desiccation and are easily destroyed in transplanting.

The literature indicates that biofilms attach on the central elongation zone, and thick biofilm formation generally occurs on the "mature root surface" (Rudrappa et al., 2008). Thus, the interest here is in how the elongation zone and mature root region are defined and how they may be identified for any given plant species. For the zone of cell

elongation, the cells in this zone stretch and lengthen as small vacuoles have the ability to fill with water. Cellular expansion in this zone is responsible for pushing the root cap and apical tip through the soil. In the Zone of Maturation the elongating cells complete their differentiation into the tissues of the primary body in this zone. It is recognized that the root hairs extend into the soil as outgrowths of single epidermal cells. They highly increase the absorptive surface of roots during the growth period when large amounts of water and nutrients are needed. Generally, an individual root hair lives for only one or two days, but new root hairs form constantly nearer the tip while old ones die in the upper part of the zone. As we know, plants can have totally different root structures but if we can define the mature root region from a simple primary root, then we can measure the mature root part in the whole root structure and thus, predict the distribution of biofilm formation on the root system.

Figure 1-4 shows the diversity of plant root systems and structures. It shows that we cannot simply define the mature root by the root shape and size, or root diameter, so we should analyze the different kinds of root systems individually. Moreover, the rhizosphere is not a region of definable size or shape, but it consists of a gradient in biological, chemical and physical properties which change both radially and longitudinally along the root (McNear et al., 2013).

Root surfaces is the substratum that provide surface area for biofilm formation and growth, thus, the variety in root surface is an indication of the variety of biofilm structure that can form on root systems. In this point, the long and dense root systems can create radically different biofilm than a short and sparse root system such as that for grass which would likely contain less active biofilm.

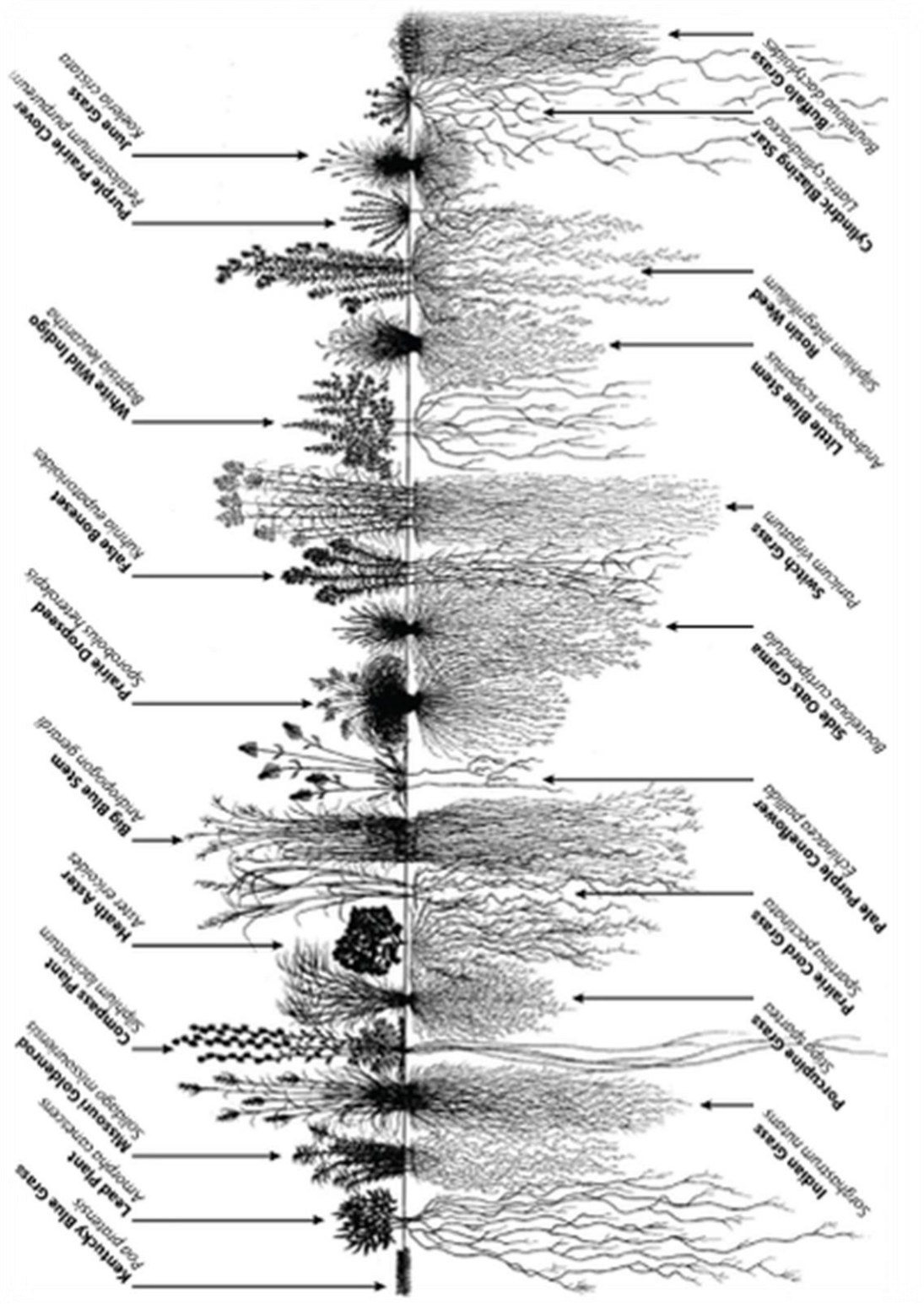

Figure 1- 4: Image shows the diversity of root system architecture in prairie plants. (David H. et. al, Nature Education, 2013)

1.5.3 The environmental factors affecting biofilm growth in the rhizosphere

Due to the dynamic nature of plant root surfaces, root biofilm initiation and development is very complex and not well understood. Soil is the main reservoir of bacterial immigrants for the potential rhizosphere community (Lakshmanan et al., 2012). In addition to physicochemical variations throughout the root surface, it is probable that other abiotic factors such as nutrient availability, temperature and relative humidity influence root biofilm associations (Lakshmanan et al., 2012). Yet, despite these challenges, diverse bacterial species have adapted to these ever-changing conditions and are capable of starting colonization by forming micro colonies on different parts of the roots from the tip to the elongation zone (Danhorn et al., 2007). Evidence is increasing that plants are able to actively select for their bacterial rhizosphere microflora, thereby creating a habitat which is most favourable for the plant. Those mciro colonies eventually grow into large population sizes on roots to form mature biofilms (Lakshmanan et al., 2012).

Compared to bulk soil, the rhizosphere is relatively rich in nutrients (Lakshmanan et al., 2012). Environmental factors include soil pH; mineral, nutrient, and water content; species, genotype, physiological state of the plant; and the presence of other microbial species, which determine the size and composition of the bacterial population sustained by the rhizosphere.

1.6 Thesis Objectives

In general, bioretention technology is applied at the macro-scale (field) scale but as the literature shows, most of the knowledge on biofilm is at the micro-level. This includes

how it is monitored and how it is modelled. Bioretention cell technology is used at the macroscale and functionality is determined generally by testing water samples at the outlet for pollutant reduction. This data does not provide direct information on whether or not, or to what degree, the biological processes are functioning to clean the water – they can only be inferred. Most applications of bioretention cell technology need predictive models of output in order to maintain them and ensure that water quality guidelines for stormwater are being met. The overall objective of the LID community is to model bioretention technology in order to implement it on as wide a field scale as possible and at the same time, be able to predict its performance. The literature above suggests that the performance of bioretention technology is directly the result of the microscale structure of the biofilm and its relationship with the vegetation root system as the root system evolves and matures. Previous research shows that the biofilm forms on the different areas of the root system. In the mature root area, the bacteria have much more nutrient in order to grow and develop. In contrast, there is no biofilm formation around the root tip part. Measurements made by laser confocal microscopes show no bacterial colonization at the root tip. Thus, in order to develop a model of bioretention technology for predictive use by those using this technology, some kind of scaling up of the modeling process is required.

Scaling-up requires a good understanding and analysis of the current mathematical models at the microscale, a means to stretch the realm of applicability to a larger scale, and the means to verify this scale-up or new model. Thus, the objectives of this thesis are to:

1. Provide a literature review of the most current and up-to-date mathematical models of substrate concentration into biofilm that are available today;
2. Analyze these mathematical models by using a sensitivity analysis to test the models' behavior to predicting both substrate and biomass concentration and how the parameters that define this behavior are affected by physical scale. Analyze these models' behavior using hypothetical data and experimental data;
3. Test the feasibility of modifying an expression for substrate flux into biofilm through the use of experimental data in conjunction with a sensitivity analysis.
4. Provide recommendations for how to structure a macro-scale model of bioretention cell's bioremediation processes.

1.7 Thesis Layout

This thesis consists of 4 chapters; Chapter 1 describes bioretention technology for stormwater quality treatment and describes the role of biofilm in bioretention cell. The introduction of biofilm formation on root surfaces is presented as well as the research objectives. Chapter 2 will offer a review of the research on the most current mathematical models for biofilm activity. It will also describe the thesis methodology including how to conduct a sensitivity analysis and what will be conducted in the subsequent chapters to achieve the objectives listed above. Chapter 3 will discuss and compare the results from the hypothetical data and experimental data, respectively. Finally, Chapter 4 gives the conclusions of this research work, and provides recommendations for future work on what are other factors that affect biofilm formation, growth and how much specific surface area on the root surface may exist in a bioretention cell.

Chapter 2: Literature Review

2.1 Mathematical Modelling of a Biofilm

Generally, because the mature root region is the larger part of a root structure, it has more biofilm; subsequently we can say that if a mature root region has a larger surface area than another mature root region, then one will observe much more biofilm on the larger surface. As previously mentioned, the root surface is the substratum for biofilm formation. More importantly, the feature of the substratum is its specific surface area *a*, or the substratum surface area divided by the system's volume. It is also associated with the substrate flux and substrate concentration, and from the substrate flux equation $J=Q(S^o-S)/aV$ (the system is at steady state) in which *J* is influenced by the specific area *a*. In addition, if the substratum is impermeable, then the substrate gradient at this location is zero. This is the starting point for how roots are to be parameterized in a model of biofilm formation.

It is necessary to give the description of a biofilm system in mathematical models, because it offers a unique approach to integrate the biological, physical, and chemical components of the biofilm system in a highly organized and structured way (Ghannoum et al., 2004). Also, the models are able to indicate sufficient understanding of the interrelations among these components governing biofilm growth and activity (Eberl, 2006). As a supplementary tool in biofilm research, mathematical models are able to make predictions of biofilm activity, systematically evaluate the importance of different parameters affecting the biofilm activity, and design the experimental approach for biofilm research.

In a biofilm model, the complexity level of a task depends on the evaluation of the biofilm problem. For example, if the research objective is to predict the flux of a limiting substrate into a flat biofilm, it will be easily done with simple biofilm models that simulate the biofilm as one-dimensional homogeneous system. By contrast, more sophisticated models are required to simulate biofilm growth in two or three dimensions when the application purpose is to mathematically reproduce the formation of complex microstructures within a biofilm (Noguera et al., 2004).

There are various biofilm models are available ranging from simple one-dimensional to complex three-dimensional models. Simple one-dimensional models focus mainly on mass diffusion through the biofilm, which can be solved analytically after some simplifications. More complex models include a set of algebraic equations describing the species distribution in biofilm and three-dimensional or dynamic models usually have a more complex structure. Each of the following models has possible applications in many suitable cases. The complexity of the model that is chosen should be depended on the application where it is used. Two or three dimensional models clearly have the advantage of including a number of the available knowledge about biofilm processes, but they have lots of unknown parameters and constants. Estimation of these parameters is very difficult, so their uses in practice are limited (Fouad et al., 2005).

Due to the limitations in computing resources available at the end of 1970s, mathematical idealization of biofilms emerged and the first conceptual models assumed biofilms to be structurally and functionally homogeneous (Noguera et al., 2004). For instance, a biofilm system is one-dimensional and defined by four elements which are substratum, biofilm matrix, boundary layer, and bulk liquid. Figure 2-1 describes the

schematic of a homogeneous biofilm system with those four elements, and L_f is the biofilm thickness and L_l is the boundary layer thickness. Mathematical modeling of this simplified biofilm system is mainly used to predict the flux of a limiting substrate from the bulk liquid to the biofilm. This problem is solved by finding the substrate concentration gradient generated within the biofilm along the direction perpendicular to the substratum. Since the substrate flux J at any location z within the biofilm is proportional to the concentration gradient at that location according to Fick's first law (Equation 7), the total flux into the biofilm is obtained from evaluating equation 7 at the surface of the biofilm.

$$J = -D_f \frac{dS_f}{dz} \qquad (7)$$

in which D_f is the diffusion coefficient within the biofilm, and S_f is substrate concentration in the biofilm.

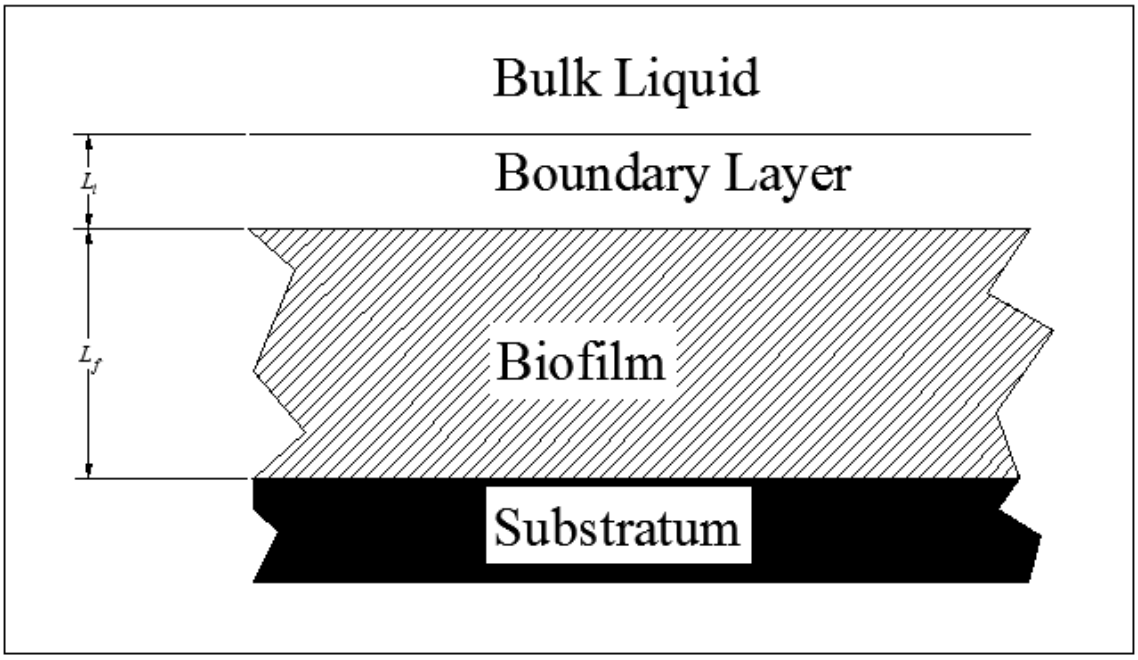

Figure 2- 1: Schematic of a homogeneous biofilm system

In the biofilm model, there are five basic processes defining biofilm activity: substrate diffusion, substrate utilization, microbial growth, decay and its distribution. In general, these basic processes in the traditional biofilm modeling are represented by partial differential equations. The equations below generally describe the processes in a biofilm modeling.

$$\frac{dS_f}{dt} = D_f \frac{d^2 S_f}{dz^2} - q \frac{S_f}{K + S_f} X_f \quad 0 \le z \le L_f \qquad (8)$$

$$\frac{dS_f}{dz} = 0 \ , \mathrm{z} = 0 \qquad (9)$$

$$D_l \frac{S_b - S_s}{L_l} = D_f \ \frac{dS_f}{dz} \ \left(when \ z = L_f\right) \qquad (10)$$

$$\frac{dX_f}{dt} = Yq \frac{S_f}{K + S_f} X_f - b' X_f \qquad (11)$$

where S_f is the substrate concentration in the biofilm, t is the time, K is the Michaelis-Menten constant, z is the co-ordinate, L_f is the biofilm thickness, D_f is the diffusion coefficient within the biofilm, D_l is the diffusion coefficient in the liquid phase, X_f is the biomass concentration with the biofilm, b is the microbial death constant, b' is the total first-order biofilm mass decay and detachment coefficient, q is the substrate consumption rate constant, S_b is the substrate concentration in the bulk liquid, S_s is the substrate concentration at the biofilm layer interface, S_1 is the substrate concentration outside the biofilm and Y is the biomass yield per unit amount of substrate consumed respectively.

Substrate utilization and diffusion within the biofilm are described by equation 8 (Ghannoum et. al, 2004), in which diffusion is represented by Fick's second law (first term on the right-hand side of the equation), and substrate utilization is represented with a Monod-type kinetic expression (second term on the right-hand side). Due to the

substratum being impermeable, so the substrate gradient at that location is zero as the boundary condition (equation 9). Equation 10 shows that the flux of substrate through the boundary layer must be equal to the flux of substrate entering the biofilm. Moreover, microbial growth is represented by a Monod-type expression (first term on right-hand side of the equation 11), and decay is represented as proportional to the biomass concentration. In addition, microbial growth equal to biofilm mass decay and detachment coefficient times biomass concentration under steady state.

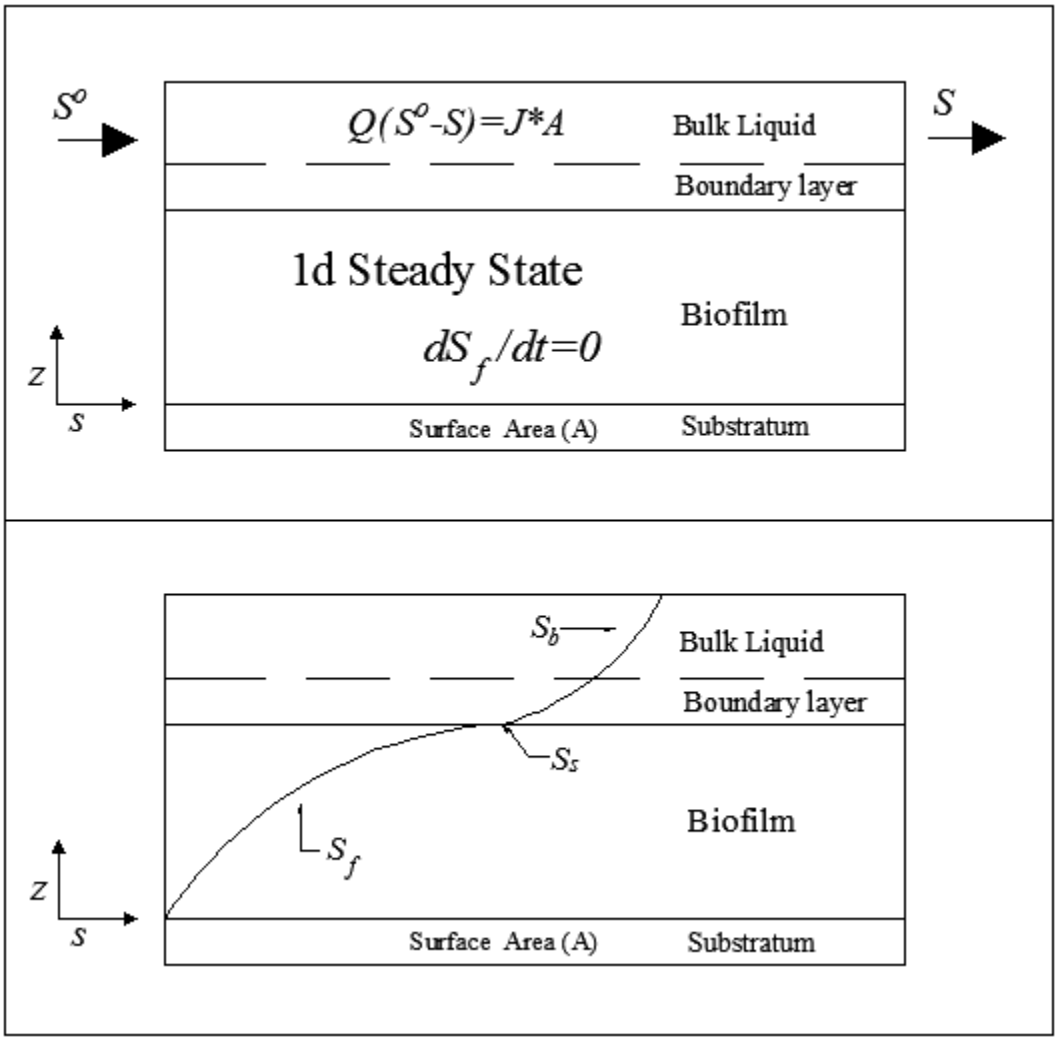

Figure 2- 2: Schematic of steady state substrate mass balance for a biofilm system

Figure 2-2 shows substrate mass balance for a steady state biofilm system in which S^o is the influent substrate concentration in the bulk liquid and S the effluent substrate concentration in the system. The substratum is the surface area that provides the area for biofilm formation, and Z is the direction along the biofilm thickness. The one dimensional steady-state problem of substrate and biomass concentration in a biofilm is considered in this present research. Thus, the substrate concentration does not change with time, and then equation 8 will equal zero under steady state conditions, then reducing to the form in equation 12. In order to ensure stability of the solution, it is assumed that the microbial death rate is proportional to the square of the biomass concentration (X_f). This square law is based on the reasoning that the death rate is not only proportional to the biomass concentration (X_f) but also to the concentration of metabolic waste products (Minkov et al., 2006). It is assumed that the substrate consumption is described by the Michaelis-Menten kinetics. Thus, the equation of balance between supply and consumption of substrate in the biofilm are presented in the following form:

$$D_f \frac{d^2 S_f}{dz^2} = q \frac{S_f}{K + S_f} X_f \qquad (12)$$

The boundary conditions are:

$$\mathrm{z} = 0, \frac{dS_f}{dz} = 0 \qquad (13)$$

$$\mathrm{z} = L_f, S_f = S_1 \qquad (14)$$

The equation for describing biomass balance is:

$$Yq \frac{S_f}{K + S_f} X_f = bX_f^2 \qquad (15)$$

From Eq.15 the concentration of active biomass can be expressed through the substrate concentration. Now Eq.12 can be written in the form:

$$D_f \frac{d^2 S_f}{dz^2} = \frac{q^2 Y}{b} \left(\frac{S_f}{K + S_f}\right)^2 \qquad (16)$$

The non-linear equation 16 is made dimensionless by defining the following variables and parameters:

$$S = \frac{S_f}{K}, x = \frac{z}{L_f}, \delta = \frac{Y q^2 L_f^2}{b K D_f}, S_L = \frac{S_1}{K} \qquad (17)$$

The Eq.16 then reduces to the following dimensionless form:

$$\frac{d^2 S}{dx^2} = \delta \left(\frac{S}{1 + S}\right)^2 \qquad (18)$$

$$x = 0, \frac{dS}{dx} = 0 \qquad (19)$$

$$x = 1, S = S_L \qquad (20)$$

The dimensionless concentration flux into the biofilm is given by

$$\psi(x) = \frac{1}{\sqrt{\delta}} \frac{dS}{dx} \Big|_{x=1} \qquad (21)$$

2.2 Solving Non-linear Differential Equations in a Steady-state Biofilm Problem by Adomin Decomposition Method

In this review part, a biofilm problem under steady state conditions is considered. Due to the character of equation 16, the non-linear differential equation is solved using the Adomian decomposition method (Muthukaruppan, 2013). As the approximate analytical expression, the solution of S(x) for substrate concentration have been derived for all values of parameters δ and S_L in equation 17, which represent the dimensionless biofilm thickness and dimensionless substrate concentration outside the biofilm, individually.

For the biofilm kinetics, there are a number of specific features. The literature describes expressions for the steady-state concentration of substrate and flux into the biofilms using the Adomian decomposition method for some selected values of biofilm thickness and substrate concentration outside the biofilm (Muthukaruppan, 2013). In addition, the biomass concentration can be solved directly by equation 15.

In order to test these expressions, Table 2-1 in section 2.4 is developed and shows values in the literature for biofilm kinetic parameters from previous studies. The ranges of values and typical values are used for simulating the results by sensitivity analysis that will be introduce in further sections.

The Adomian decomposition method is typically applied to linear and nonlinear problems. The most important advantage of this method is that it provides a rapid convergent series solution. However, in this method, some modifications are proposed by several authors (Jaradat 2008, Wazwaz et al., 2004, Makinde 2007, Biazar et al., 2004, Siddiquia et al., 2010 and Mohamed 2010). The Adomian decomposition method is an extremely simple method to solve the non-linear differential Equations. Moreover, the obtained result is of high accuracy. The solution of equation 18 is solved by this method, and an approximate analytical expression of concentrations S(x) is given in the Eq.22.

$$S(x) = S_L + \frac{\delta}{2}\left(\frac{S_L}{1+S_L}\right)^2(x^2-1) + \frac{\delta^2 S_L^3}{(1+S_L)^5}\left(\frac{x^4}{12} - \frac{x^2}{2} + \frac{5}{12}\right)$$

$$+ \frac{\delta^2 S_L^4}{4(1+S_L)^6}\left(\frac{x^6}{30} - \frac{x^4}{6} + \frac{x^2}{2}\right) - \frac{\delta^2 S_L^5}{(1+S_L)^7}\left(\frac{x^6}{30} - \frac{x^4}{6} + \frac{x^2}{2}\right)$$

$$+ \frac{2\delta^2 S_L^5}{(1+S_L)^7}\left(\frac{x^6}{360} - \frac{x^4}{24} + \frac{5x^2}{24}\right) + \frac{3\delta^2 S_L^6}{4(1+S_L)^8}\left(\frac{x^6}{30} - \frac{x^4}{6} + \frac{x^2}{2}\right)$$

$$- \frac{2\delta^2 S_L^5}{(1+S_L)^8}\left(\frac{x^6}{360} - \frac{x^4}{24} + \frac{5x^2}{24}\right)$$

$$+\frac{\delta^2 S_L^4}{360(1+S_L)^8}(-155+66S_L) \qquad (22)$$

The solution of concentration flux into the biofilm is obtained as:

$$\psi=\frac{1}{\sqrt{\delta}}[\delta(\frac{S_L}{1+S_L})^2-\frac{2}{3}\frac{\delta^2 S_L^3}{(1+S_L)^5}+\frac{2}{15}\frac{\delta^2 S_L^2}{(1+S_L)^6}-\frac{8}{15}\frac{\delta^2 S_L^5}{(1+S_L)^7} \qquad (23)$$

$$+\frac{8}{15}\frac{\delta^2 S_L^4}{(1+S_L)^7}+\frac{2}{5}\frac{\delta^2 S_L^6}{(1+S_L)^8}-\frac{8}{15}\frac{\delta^2 S_L^5}{(1+S_L)^8}]$$

2.3 Two Selected Models for Substrate Flux J into Biofilm

This part is carried out to simplify existing biofilm one-dimensional models, which consider a single substrate as the limiting factor. Two models: (1) Suidan and Wang model (1985) and (2) Sáez and Rittmann model (1988, 1992), are selected for this research. Moreover, both of these models have modified expressions and exact solutions, and they are short and easy to use giving reliable results in comparison to the original models (Fouad et al., 2005).

The previous study of mathematical models has shown that the various biofilm-kinetic models are not widely used in general practice, except the simple and empirical forms (Sáez and Rittmann 1990). Thus, the simplified one-dimensional biofilm models are considered and used for simulation and study of biofilm systems in many applications. These models, which are based on Monod kinetics and Fickian diffusion law, have been studied by many researchers (Fouad et al., 2005). Also, they have confirmed that equations in the models have no explicit solution, except for some limiting cases (Fouad et al., 2005).

Based on this set of equations in the first model, (1) Suidan and Wang (1985) has assumed first order kinetics and proposed the following equation to express the dimensionless substrate flux (J^*) into the biofilm for each value of $S^*>S^*min$:

$$S^* = J^* L_f^* + \frac{0.5J^{*2} + J^*[1.0 + \left(\frac{J^*}{3.4}\right)^{1.19}]^{-0.61}}{\tanh(\frac{J^*}{S_{min}^*})} \qquad (24)$$

where L_f^* is the dimensionless thickness of the stagnant layer, S^* is the dimensionless effluent substrate concentration, and S_{min}^* is the dimensionless minimum substrate concentration that can sustain biofilm.

For the same condition ($S^*>S_{min}^*$), the (2) Sáez and Rittmann model (1988, 1992) has also presented the following set of parametric equations, which gives a unique value of J^* for each value of S^*.

$$S^* = S_s^* + J^* L_f^* \qquad (25)$$

$$J^* = f J_{deep}^* \qquad (26)$$

$$f = \tanh\left[\alpha\left(\frac{S_s^*}{S_{min}^*} - 1\right)^{\beta}\right] \qquad (27a)$$

$$\alpha = 1.5557 - 0.4110\tanh(logS_{min}^*) \qquad (27b)$$

$$\beta = 0.5035 - 0.0257\tanh(logS_{min}^*) \qquad (27c)$$

$$J_{deep}^* = [2(S_s^* - ln(1 + S_s^*))]^{0.5} \qquad (28)$$

in which S_S^* is the dimensionless minimum substrate concentration at the diffusion layer, f is the ratio between flux into actual and deep biofilm, α and β are product and exponential coefficients, respectively, in the expression for factor f (eq.27a), and J_{deep}^* is the dimensionless substrate flux into deep biofilm.

These two selected models are the most widely accepted models for practical applications. They allow one to estimate the substrate flux into the biofilm and the expected steady-state biofilm thickness without the need to calculate substrate gradients within the biofilm (Goudar et al., 2002, Noguera et al., 2004). They calculate a number of dimensionless parameters, and then solving algebraic equations (eq.25-28) that represent the flux of substrate through the boundary layer and into the biofilm. The two previous models have no explicit solutions for J^*. Suidan et al. (1989) for the first model and Heath et al. (1990, 1991) for the second have developed graphical solutions (Fouad et al., 2005). The plotted figures from exact solution of the second model and the approximated expression in first model are compared in Chapter 3. The graphical solutions of these two models are prepared for some selected values of L_f^* and S_{min}^* which are useful for sensitivity analysis.

2.3.1 Modified Expression of the Suidan and Wang Model (1985)

In order to obtain the solution to Suidan and Wang model, amount of attempts have been made to rearrange equation 24 in a simple form. However, the exact solution of equation 24 is still not found, but the following equations give the approximated expressions that have been developed:

$$S^* = 1.3J^{*1.76} + (L_f^* J^*)^{0.88} + S_{min}^* \; for \; S_{min}^* < 10.0 \qquad (29a)$$

$$S^* = L^* J^* + S_{min}^* (0.45J^* + 1) \; for \; S_{min}^* \geq 10.0 \qquad (29b)$$

Equations (29a) and (29b) have explicit solutions as follows:

$$J^* = \left(\frac{\left[\sqrt{\left(L_f^*\right)^{1.76} + 5.2(S^* - S_{min}^*)} - \left(L_f^*\right)^{0.88}\right]}{2.6}\right)^{\frac{1}{0.88}} for \; S_{min}^* < 10.0 \quad (30a)$$

$$J^* = \frac{(S^* - S^*_{min})}{0.45S^* + L^*_f} for\ S^*_{min} \geq 10.0 \qquad (30b)$$

2.3.2 The Exact Solution of the Sáez and Rittmann Model (1988, 1992)

Sáez and Rittmann model was considered in a parametric form (Fouad et al., 2005). Thus, it is suggested to cancel the parameter S^*_s which can lead to an explicit equation. Many procedures of pure mathematics have been done to modify this set of equations (Fouad et al., 2005). Finally the following quadratic equation, which represents the exact solution of this set, has been obtained.

$$S^* = 0.5J^{*2} + L^*_f J^* + S^*_{min} \qquad (31)$$

Equation (31) can be rewritten in simple dimensional form as:

$$Lo = \frac{L_f J}{D_w} + \frac{0.5J^2}{K_m X_f D_f} + S_{min} \qquad (32)$$

where D_f is the substrate's diffusion coefficient in the biofilm, D_w is the molecular diffusion coefficient in water, J is the substrate flux into biofilm, K_m is the maximum specific rate of substrate utilization, K_d is the specific decay rate, K_s is the Monod half-velocity coefficient, Lo is effluent substrate concentration, L_f is biofilm thickness, and S_{min} is the minimum substrate concentration that can sustain biofilm, which is equal to K_s/(YK/b_t -1), and X_f is the biofilm microbial density, and Y is yield coefficient and b_t is the first order decay and shear loss rates.

The solution of equations [31] and [32] are:

$$J^* = [L^{*2}_f + 2(S^* - S^*_{min})]^{0.5} - L^*_f \qquad (33)$$

$$J = [\left(L_f K_m X_f \frac{D_f}{D_w}\right)^2 + 2K_m X_f D_f (Lo - S_{min})]^{0.5} - L_f K_m X_f \frac{D_f}{D_w} \qquad (34)$$

2.4 Methodology

The five research objectives stated in section 1.6 are achieved in this thesis through the following methodology: The literature review noted in sections 2.1 – 2.3 achieve objective 1. Objective 2 and 4 regarding sensitivity analysis are achieved by the methodology described in section 2.4.1 below. Objectives 3 and 4 are achieved by the methodology described in section 2.4.2. The recommendations for future research are given in chapter 4 (objective 5).

Sensitivity analyses methods are need to determine how the uncertainty in the output of a mathematical model or system can be divided to different sources of uncertainty in its inputs. In other words, the main purpose of a sensitivity analysis is to recalculate outcomes under alternative inputs and parameters to determine which factors influence the variation in the results. Generally, a mathematical model is defined by a series of equations, inputs and kinds of parameters, and it is hard to understand the relationship between input and output in highly complex models. Thus, sensitivity analyses address by how much the input contributes to the output uncertainty and describes the relevance of the input effect on the outcomes.

2.4.1 Sensitivity Analysis Involving Solutions to the Substrate and Biomass Concentration.

In modeling, the kinetic parameters and variables are very important, and it is necessary to define the values for the parameters that are included in the model. This is because the values of model parameters can significantly affect modeling results. A literature review was performed for possible values for kinetic model constants, and parameters that influence the solutions of substrate concentration and biomass concentration (see Table 2-1). Sometimes, a large change in the value of a parameter has

no effect on the model output while a small change in a parameter value has a significant impact in some other situations. Sensitivity analysis is typically used to determine which parameter has a large, small or no influence on the model outputs. This provides input on which parameters must have highly accurate values, while other parameters can be around a "reasonable range". Based on this literature research, typical kinetic parameters in the previous model studies were used, and the substrate concentration in the solution was tested by experimental data and typical values when the biofilm parameters were fixed such as biofilm thickness. Typically, a change in the substrate concentration outside the biofilm S_1 within a typical range from 0.0005 to 0.05 mg/cm^3 leads to the variable S_L in the equation to change from 0.05 to 5, and this change is due to the fixed the Michaelis-Menten K constant for 0.01 mg/cm^3. The concentration of NO_3^- from the outlet in the bioretention cell was used as the experimental data, and the data was selected from the different seasons during three years of experimentation by Khan (2011). In this case, we are going to test the solutions for both substrate and biomass concentration by the experimental data, and compare the results between hypothetical values and experimental values.

Typical kinetic model constants are the substrate consumption rate constant, the Michaelis-Menten constant, the biomass yield coefficient, the Microbial death constant and the diffusion coefficient within the biofilm. The model will run all model parameters at their typical values and the selected range values from minimum and maximum for sensitivity analysis. The sensitivity of the model to variations in each of the kinetic model constants from table 2-1 are calculated by equation 15 and 22. In chapter 3, it offers the

discussion on the impact of those parameters in the steady-state biofilm model. All the biofilm kinetic parameters are from the literature review in previous studies.

Parameters	Range of Values	Typical Value	Units	Reference	Minimum	Maximum
q		10	day^{-1}	Noguera et al. (2004)	1	10
K	0.0066-0.018	0.01	mg/cm^3	Meima et al. (2008)	0.001	0.02
Y	0.24-0.63	0.5	mg/mg	Noguera et al. (2004)	0.1	1
b	0.05-1.2	0.1	$cm^3/mg*day$	Meima et al. (2008)	0.01	1
Df/Dl	0.2-0.9	0.8		Noguera et al. (2004)		0.8

Table 2-1: Literature overview of kinetic model constants, including range of values, typical values, minimum and maximum parameter values used in the sensitivity analysis

There is no literature on values for stormwater to the author's knowledge. Table 2-2 gives an example, which considers a specific wastewater having the kinetic coefficients in a completely mixed process (Fouad et al., 2005).

Parameters	Value	Units	Reference
q	10	day^{-1}	Fouad et al. (2005)
K	0.01	mg/cm^3	Fouad et al. (2005)
Y	0.45	mg/mg	Fouad et al. (2005)
b	0.1	$cm^3/mg*day$	Fouad et al. (2005)
D_f	0.75	cm^2/day	Fouad et al. (2005)
X_f	25	mg/cm^3	Fouad et al. (2005)
b_t	0.41	day^{-1}	Fouad et al. (2005)
L_f	0.0078	cm	Fouad et al. (2005)
D_w	1.25	cm^2/day	Fouad et al. (2005)
Km	10	day^{-1}	Fouad et al. (2005)

Table 2- 2: The kinetic coefficients in a specific wastewater process

2.4.2 Testing Solutions with Real World Data and Determining Reasonable and Practical Ranges.

Model variables that were input in the sensitivity analysis included substrate concentration inside and outside of the biofilm, and biofilm thickness. A sensitivity analysis of the model variations in the parameters shown in Table 2-1 will be conducted. The research will use existing biofilm one-dimensional models, which consider a single substrate (effluent substrate concentration of the biofilm) as the limiting factor. In addition, the models of (1) Suidan and Wang (1985) and (2) Sáez and Rittmann model (1988, 1992) were selected for the study. The results of modified expressions of (1) model and the exact solution of (2) model are compared to the two original models running the same biofilm kinetics parameters. In order to determine the reasonable and practical range of the substrate flux, the proposed expression of substrate flux into the biofilm (equation 34) was selected and tested with both hypothetical data and experiment data.

BOD and Nitrate data are selected as the test experimental data for substrate flux *J* and substrate concentration into the biofilm, respectively. The difference between inlet substrate concentration and outlet substrate concentration calculated tell us how much biomass concentration changes in a biofilm and how much substrate flux goes into a biofilm based on experimental data. Based on the mathematical modeling in this study, we use typical values for other parameters in the equations and some fixed values are chosen in the modeling, because they are difficult to measure and uncontrolled. The experimental data were collected in the spring (Sp), summer (S), fall (F), and winter (W) (Khan, et. al, 2011).

Two mathematical models for nitrification and BOD concentration processes in the solutions of substrate concentration and substrate flux were developed. In the biofilm model, parameters evaluated include kinetic parameters and also biofilm parameters and biofilm variables, such as biofilm thickness, biomass concentration and the substrate concentration inside and outside of the biofilm.

BOD is used to determine what affect both wastewater and storm water containing organic materials, will have on oxygen abundance in receiving water because the bacteria will take in oxygen in order to breakdown these molecules. Thus if bacteria are taking in large amounts of oxygen, this will have a disadvantageous effect on the surrounding ecosystem. Thus, BOD is a surrogate for biological activity related to decomposition of organic material. The concentration of ultimate BOD or BOD_u was used as the effluent substrate concentration (L_o) in the simulation. Generally, BOD_5 is approximately two-thirds of ultimate BOD in most wastewater, but it is not usually used in stormwater due to the smaller amount of organics in stormwater. In this case, the BOD_5 data was selected from the different seasons in the past site experiment, then ultimate BOD was calculated from the BOD_5.

Parameters	Value	Units	Reference
q	10	day^{-1}	Noguera et al. (2004)
K	0.01	mg/cm^3	Noguera et al. (2004)
Y	0.24	mg/mg	Noguera et al. (2004)
b	0.1	$cm^3/mg*day$	Noguera et al. (2004)
D_f	0.64	cm^2/day	Noguera et al. (2004)

Table 2- 3: Summary of parameters used for experimental test (NO_3^-) by equation 15 and 22.

Parameters	Value	Units	Reference
q	10	day^{-1}	Minkov et al. (2006)
K	0.01	mg/cm^3	Minkov et al. (2006)
Y	0.45	mg/mg	Minkov et al. (2006)
b	0.1	$cm^3/mg*day$	Minkov et al. (2006)
D_f	0.75	cm^2/day	Minkov et al. (2006)

Table 2- 4: Summary of parameters used for experimental test (BOD_u) by equation 34

Table 2.1 generally gives the range for kinetic parameters which can be used for different kinds of water Tables 2.3 and 2.4 are for testing nitrate and BOD because the yield coefficient (Y) of 0.24 is for nitrifiers set to 0.45 for BOD. Finally, the Table 2.2 gives the parameters from a specific wastewater, which is a synthetic form of domestic wastewater. Therefore, this table is for simulation or prediction use only.

Chapter 3: Results and Discussion

3.1 Sensitivity of Biofilm Kinetic Parameters in the Model

Table 2-1 describes the literature overview of kinetic model constants, and those values include a range of values, typical values, minimum and maximum parameter values. In addition, it is suggested to ignore the detachment rate (b_{det}) because its value is very small, and this is main reason that the value of b is close to b' or equal to b' in some conditions. In our simulation, there is limited experience for b from previous studies in stormwater, so we tested the range of values and typical values to see how much it affects the results. Michaelis-Menten kinetics is the model of enzyme kinetics which is related to enzymatic reactions. Generally, biochemical reactions involving a single substrate are often assumed to follow Michaelis-Menten Kinetics (Minkov et al., 2006). K is the substrate concentration at which the reaction rate is half of the maximum velocity. The solution of substrate concentration S(x) is based on the theory of enzymatic reaction and this K is presented as that of Michaelis-Menten. There are three parameters which include microbial death constant (b), biomass yield coefficient (Y) and Michaelis-Menten constant (K) that are tested in some selected values. They are used in the sensitivity analysis by running equation 22.

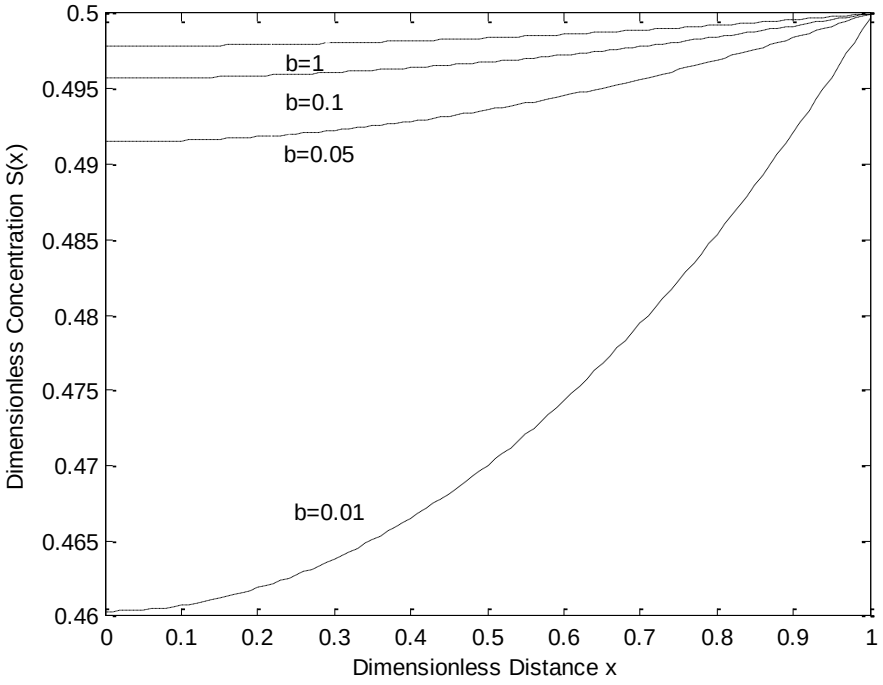

Figure 3- 1: Sensitivity analysis of model parameter for various values of *b*

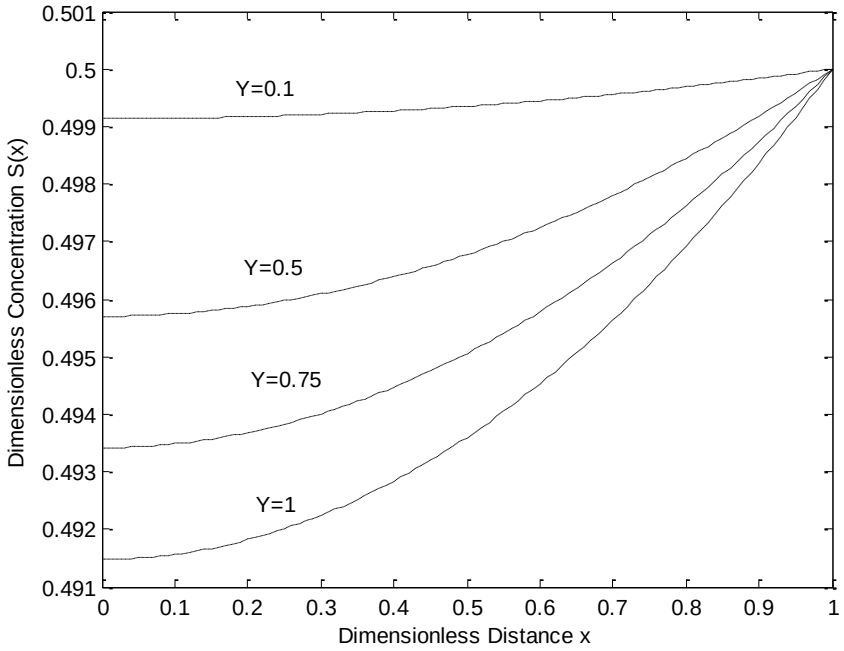

Figure 3- 2: Sensitivity analysis of model parameter for various values of *Y*

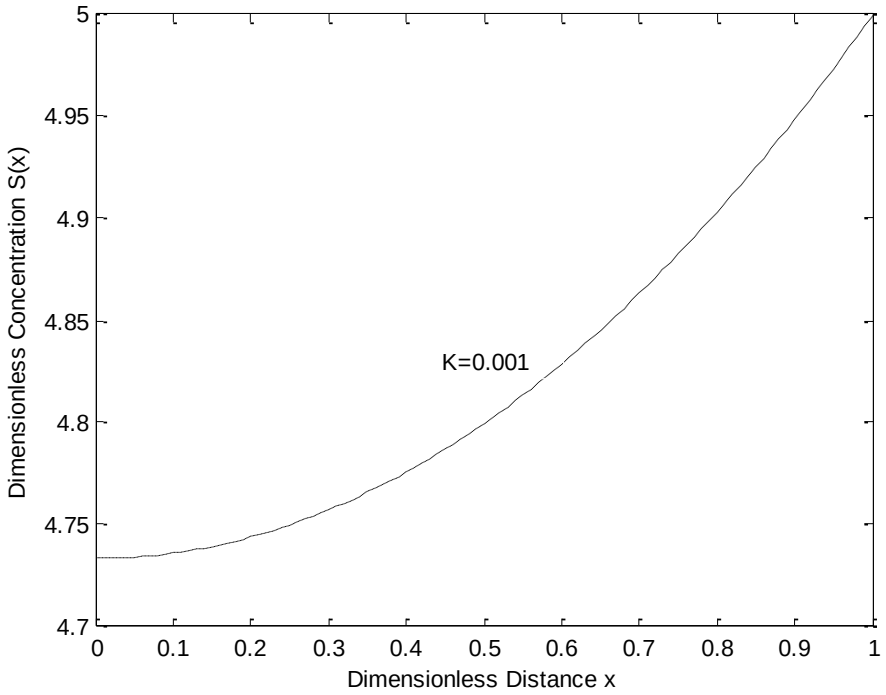

Figure 3- 3: Sensitivity analysis of model parameter for K = 0.001

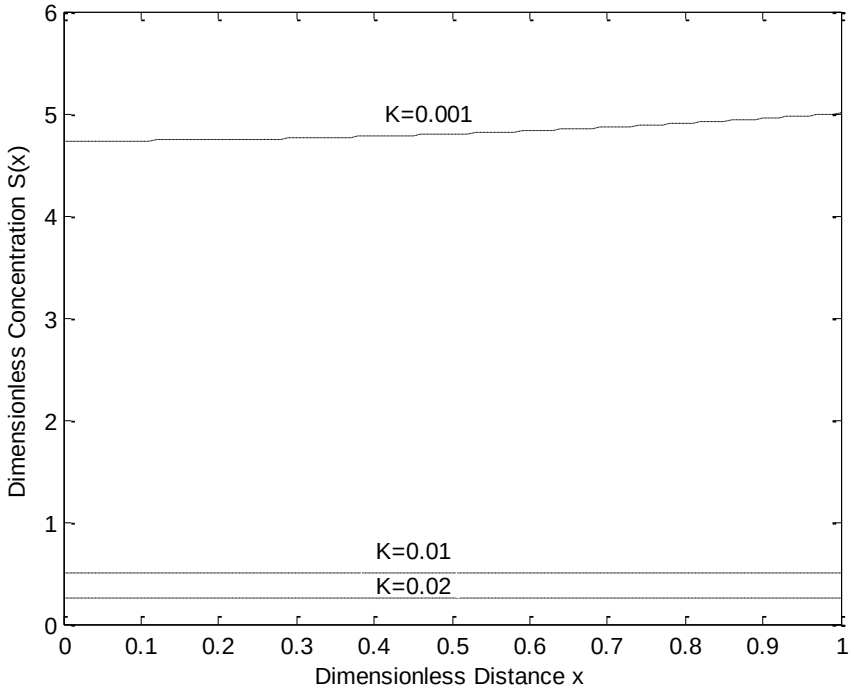

Figure 3- 4: Sensitivity analysis of model parameter for K = 0.001, 0.01 and 0.02, when S_L=5, S_L=0.5 and S_L=0.25

Based on the initial conditions, the dimensionless distance is range from 0 to 1, which represents the distance from the start of biofilm at the substratum or root surface to the end of biofilm at the boundary layer. Figure 3-1 shows the substrate concentration will increase slightly while microbial death constant *b* is close to 1, however, as the dimensionless distance *x* goes up, the substrate concentration value will significantly grow while microbial death constant offers a low value at 0.01. Figure 3-2 shows that the biomass yield coefficient does not influence the substrate concentration because the substrate concentration stays at the same level even if the value of *Y* is close to 1. Figure 3-3 shows there is an upward trend for the substrate concentration when the dimensionless distance is rising during the minimum K=0.001. Figure 3-4 illustrates various values of *K* has a large effect on the results of the substrate concentration S(x), this is due to this value being strongly related to the initial conditions (S_L, S_1) in the model in equation 17, thus, it needs careful selection. For further estimates, the value of biofilm thickness is considered by comparing between 0.001 cm and 0.01 cm and for the substrate concentration in the liquid, S_1 =0.005 mg/cm^3. At these values, δ =0.0375 and 3.75, and S_L =0.5. Other parameters follow the value in table 2-1 for simulating the results of the substrate concentration.

3.2 Sensitivity of Substrate and Biomass Concentration

The solution of concentration S(x) is plotted by equation 22, and the simulation results show that concentration S(x) for various values of *x* (from 0 to 1) and when fixed some values of S_L. The results are presented in the following figures for some selected values of dimensionless biofilm thickness δ and dimensionless substrate concentration outside of the biofilm S_L. Figures 3-5 to 3-7, it is evident that the value of concentration gradually

increases as the dimensionless biofilm thickness δ decreases. Figures 3-8 to 3-10 represent the concentration S(x) for various values of S_L. From these figures it is observed that, the value of the concentration increases when S_L increases. When $\delta \leq 1$, the value of concentration is stable at the same level and its value depends upon S_L. On the other hand, it is clear to know that as dimensionless substrate concentration outside the biofilm S_L increases, then the value of dimensionless concentration S(x) increases. Eq.23 represents the normalized concentration flux into the biofilm. Figure 3-11 represents flux versus S_L (dimensionless substrate concentration outside the biofilm). From this figure, it is predicted that the value of concentration flux decreases when the thickness of biofilm increases. The following figures are plotted by the Matlab® program.

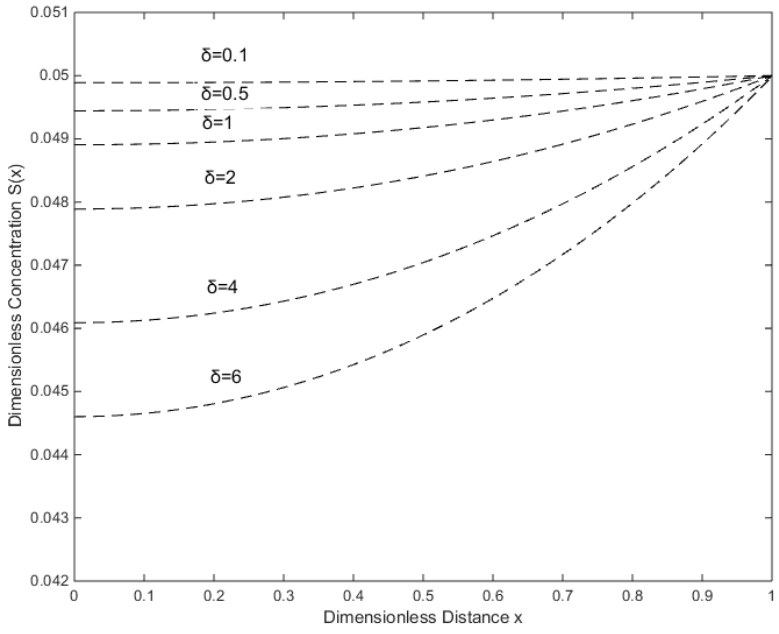

Figure 3- 5: The concentration S(x) were computed for various values of δ when fixed the value of S_L=0.05.

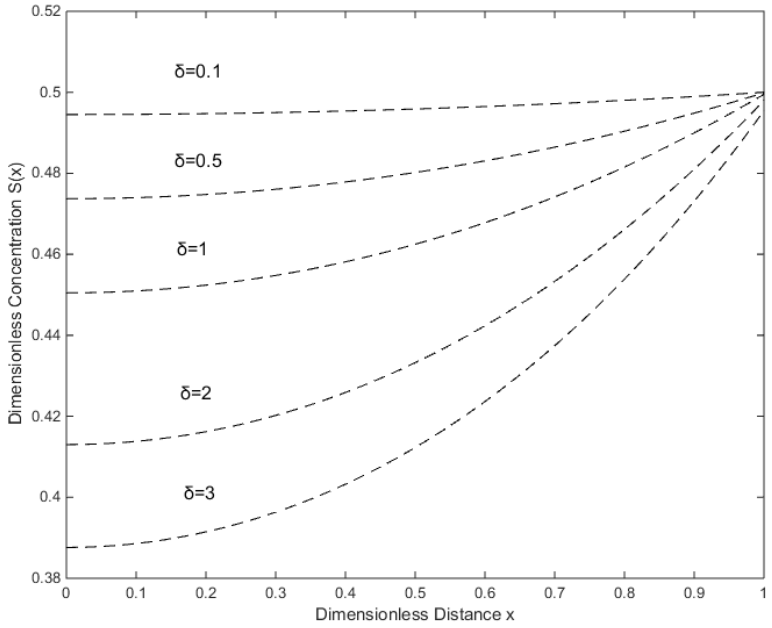

Figure 3- 6: The concentration S(x) were computed for various values of δ when fixed the value of S_L=0.5.

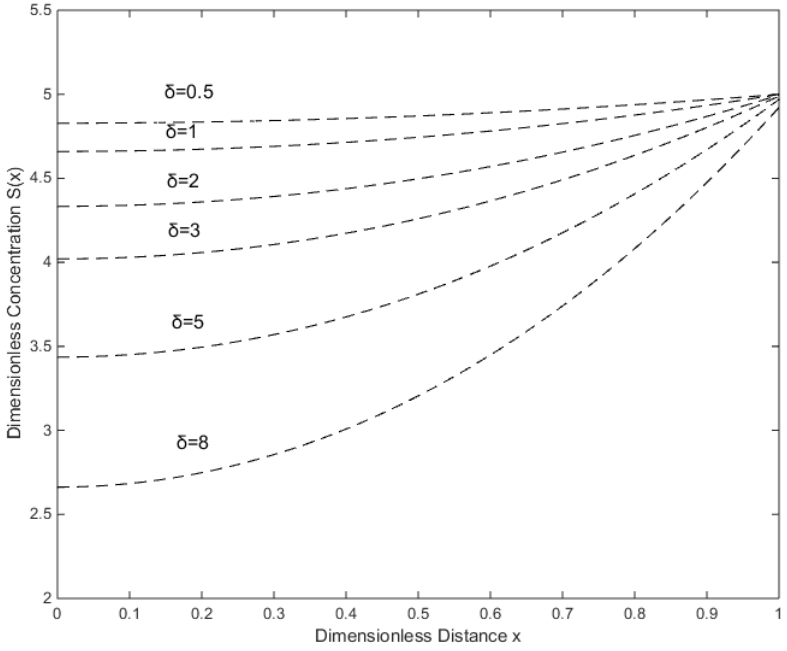

Figure 3- 7: The concentration S(x) were computed for various values of δ when fixed the value of S_L=5.

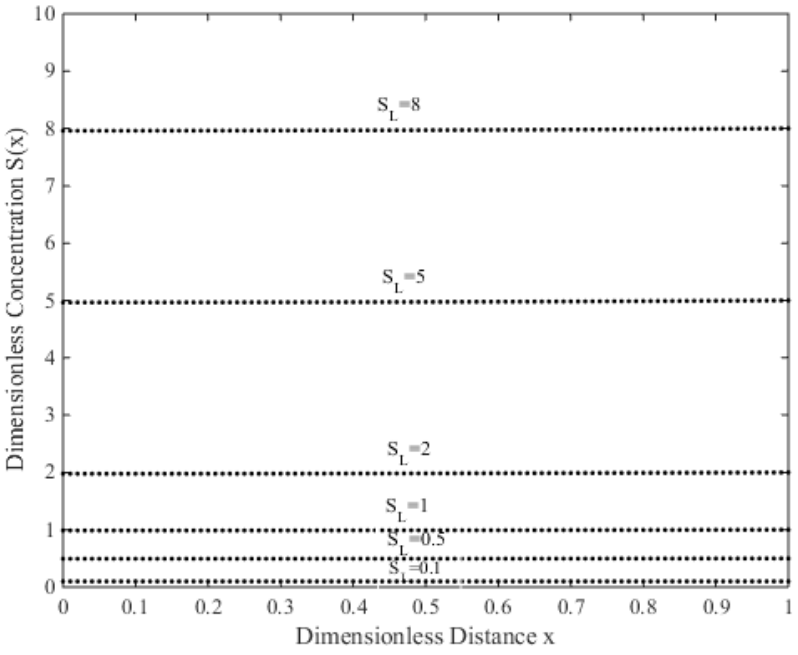

Figure 3- 8: The concentration S(x) were computed for various values of S_L when fixed the value of δ =0.1.

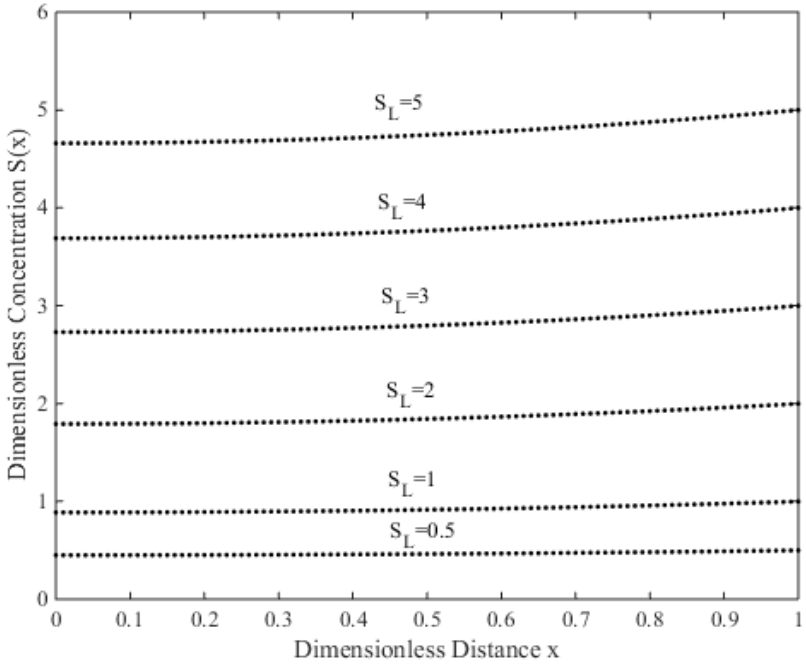

Figure 3- 9: The concentration S(x) were computed for various values of S_L when fixed the value of δ =1.

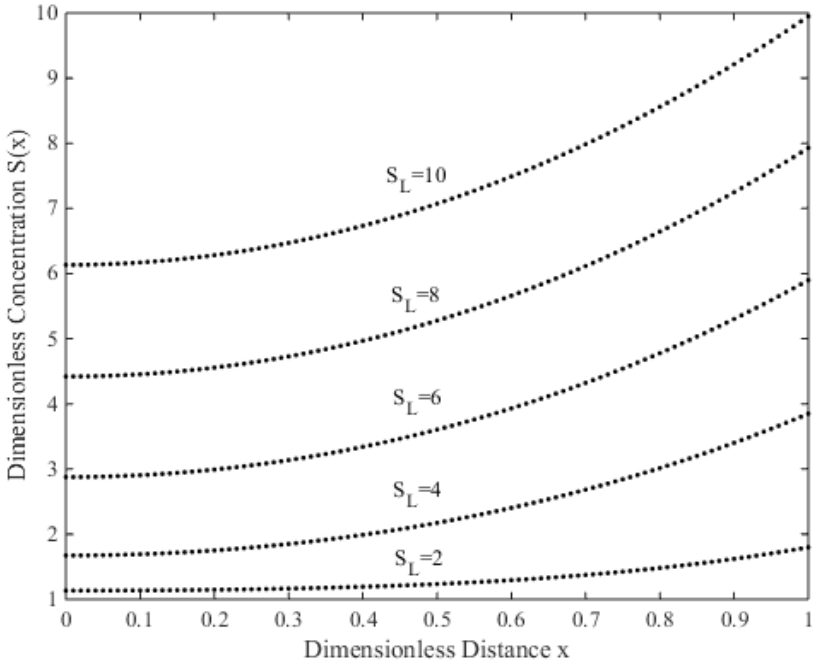

Figure 3- 10: The concentration S(x) were computed for various values of S_L when fixed the value of δ =10.

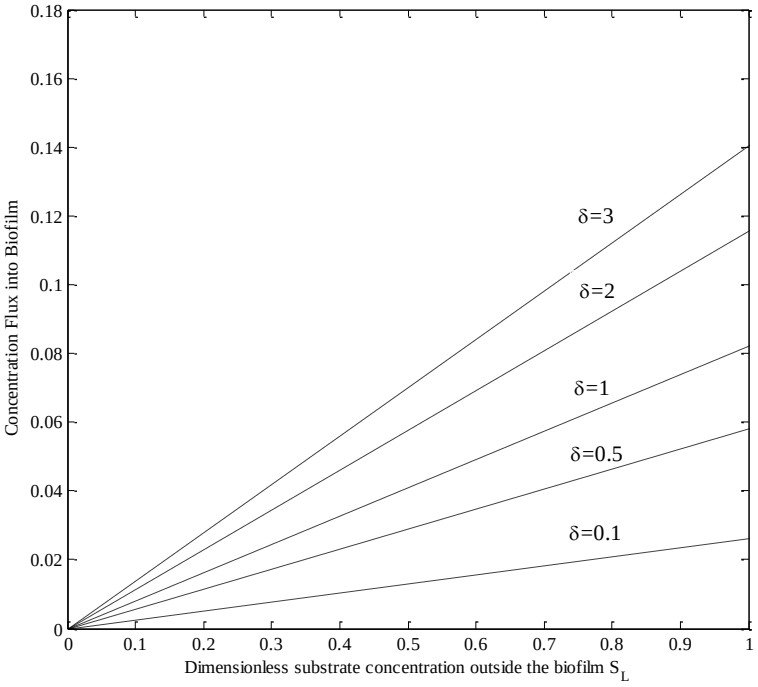

Figure 3- 11: The concentration flux into biofilm was computed for various values of δ.

From figure 3-5, it is clear to see that the value of concentration decreases slightly for a fixed small value of S_L and the dimensionless biofilm thickness δ increases quickly. In the figure 3-6 and 3-7, the value of concentration falls significantly due to an increase of ten times the value of $S_{L.}$ However, as the dimensionless distance x goes up, the concentration S(x) stays at a stable value when the dimensionless biofilm thickness is fixed. Thus, the values of biofilm thickness and S_L are the main factors that affect the results of concentration S(x). In this case, we fixed the value of biofilm thickness while changing various values of S_L, the last three figures illustrate that the concentration goes down very fast even if we increase by ten times the value of biofilm thickness. It is noted that S_L is the dimensionless substrate concentration outside the biofilm, and the results of concentration S(x) represents the dimensionless substrate in the biofilm; therefore, in the steady state conditions we can predict the concentration S in the biofilm by changing the experimental data for S_L.

3.2.1 Experimental Data Discussion on Substrate and Biomass Concentration

From the sensitivity analysis the solution of concentration S(x) for changing the various values of dimensionless biofilm thickness δ and dimensionless substrate concentration outside the biofilm $S_{L,}$ it is evident that those parameters have different effect on the results of concentration S(x). In order to test experimental data, typical kinetic parameters in the previous model studies are used (Table 2-2), and the biofilm parameters such as biofilm thickness of 0.01cm and 0.001cm, are selected individually. For the experimental data, the concentration of nitrate from the outlet in the bioretention cell was used as the substrate concentration in the liquid, and the data was selected from the different seasons (Khan, 2011).

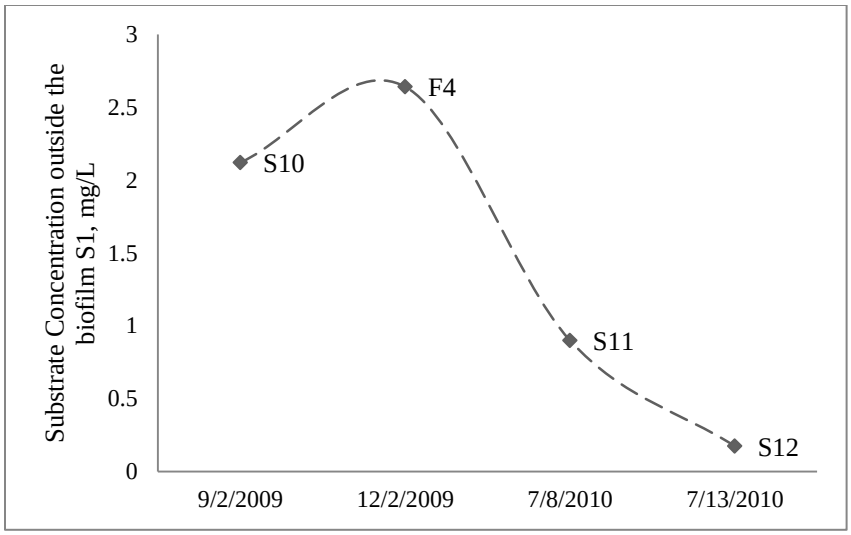

Figure 3- 12: Selected experimental data for various values of the concentration S_L in the liquid

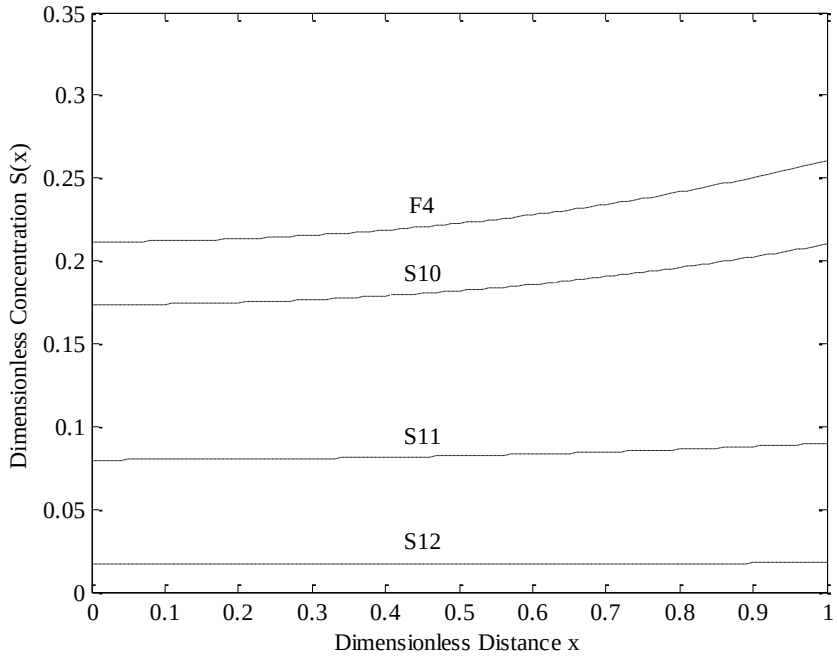

Figure 3- 13: The concentration S(x) were computed for various values of the experimental data for S_L when fixed the value of δ =3.75 and L_f=0.01.

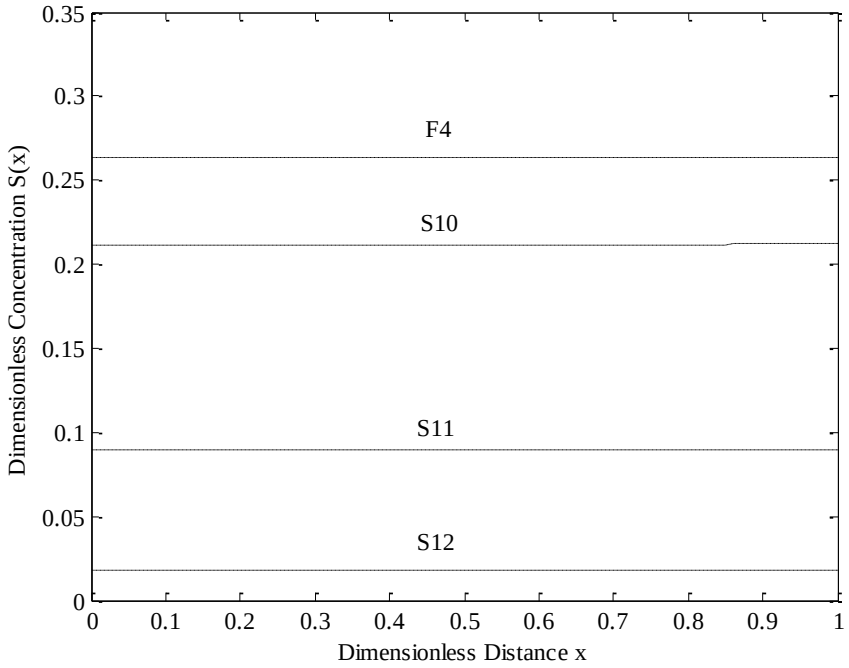

Figure 3- 14: The concentration S(x) were computed for various values of the experimental data for S_L when fixed the value of δ =0.0375 and L_f=0.001.

Figure 3-12 shows the data for various values of the dimensionless concentration outside the biofilm S_L. Figure 3-13 and Figure 3-14 illustrates the model results for fixed biofilm thickness of 0.01cm and 0.001cm, which leads to values of δ of 0.0375 and 3.75, respectively. There is no effect on the value of concentration S(x) when the dimensionless distance grew in the Figure 3-14, because once $\delta \leq 1$, the concentration is stable at a uniform value, and its value depends upon S_L; However, the results of concentration S(x) in those two figures stayed at the same level; around 0.05 to 0.35.

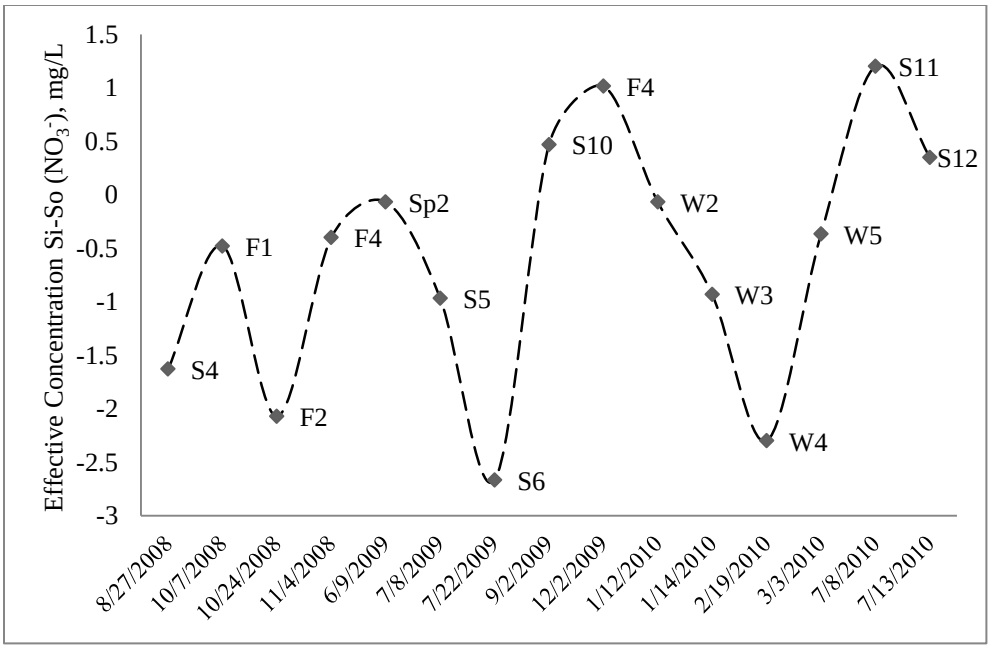

Figure 3- 15: Selected experimental data for effective concentration *Si-So* (NO_3^-).

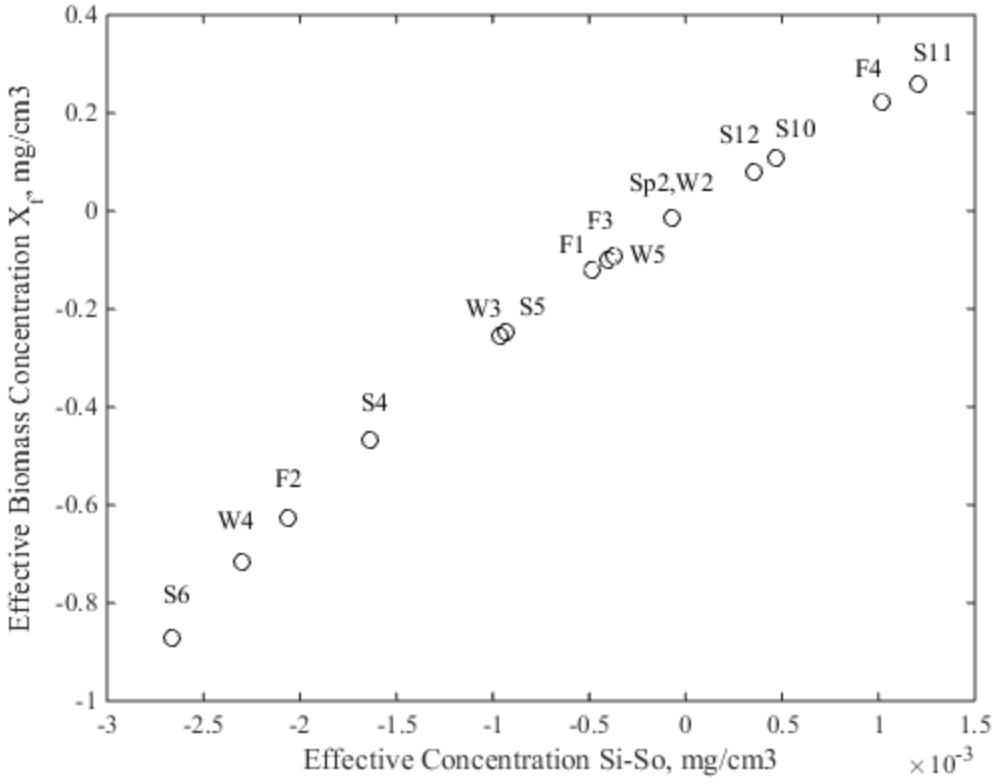

Figure 3- 16: The effective biomass concentration X_f was computed for various values of the effective concentration *Si-So* (NO_3^-).

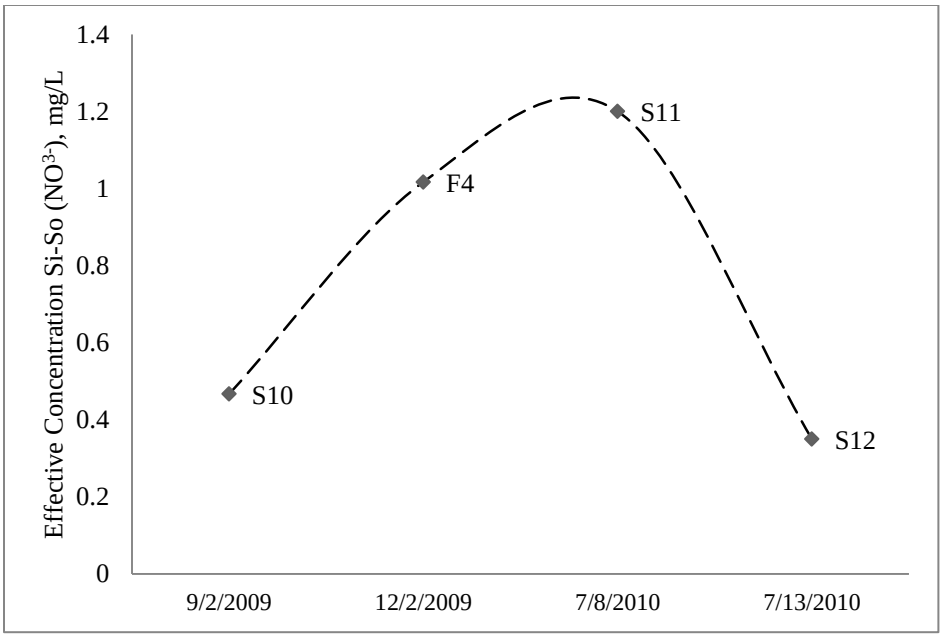

Figure 3- 17: Production effective concentration Si-So from experimental data (NO_3^-).

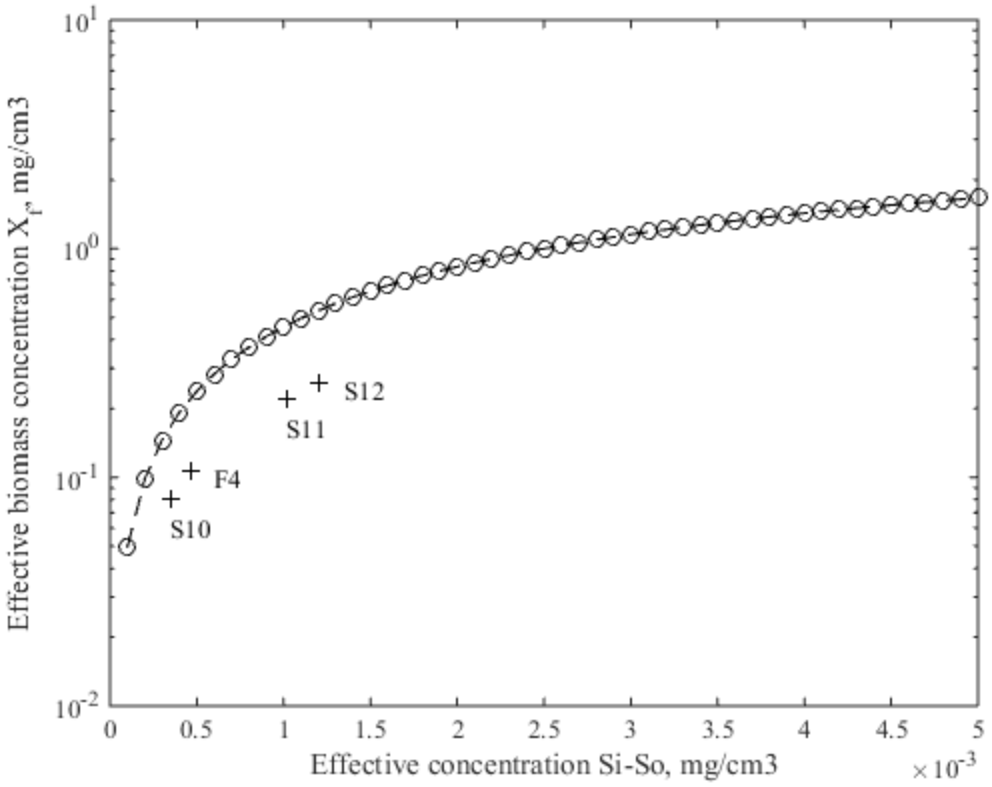

Figure 3- 18: The effective biomass concentration X_f was tested by typical value and experimental data of the effective concentration *Si-So* (NO_3^-).

Figure 3-15 describes the various values of effective substrate concentration, represented by *(Si-So)* where *Si* and *So* are the substrate concentration inside and outside the biofilm, respectively. Figure 3-16 is plotted using equation 15, which shows the effective biomass concentration changed with different seasonal data. It is noted that the effective substrate concentration and biomass concentration are supposed to have a positive value, thus, production in the experiment data is showing in Figure 3-17. In this case, the value of effective biomass concentration should be positive because the biofilm group are growing in that period. Thus, it is predicted that the biological processes will occur in the summer term, some factors such as temperature, climate and plant growth in that season may influence the prediction results. Finally, the hypothetical data is tested using the equation (15) and Figure 3-18 gives the comparison between effective biomass concentration using experimental data and hypothetical data.

The solutions of the model address the relationship between substrate concentration in the biofilm and outside the biofilm when we fix some values of biofilm thickness. The figures above presented the results of both substrate concentration and biomass concentration by testing the hypothetical data and experiment data.

3.3 Sensitivity of Modified expression for substrate flux J into biofilm

The proposed equations (31), (32), (33), or (34), which represent the exact, explicit, and dimensional models of biofilm, are a very useful and helpful for other purposes such as describing the biofilm performance as opposed to a simple graphical solution and for evaluating the biofilm kinetics parameters in the model. Moreover, it is also a beginning step to simplifying other complex biofilm models in future research.

Figures 3-19 to 3-23 illustrate the similar results from both (eq.31) and (eq.33). The results have been plotted corresponding to a number of different values of L_f^* (from 1 to 50) and S_{min}^* (from 0.025 to 1000) to ensure the validity of the proposed equation. The explicit solution of equation (30a) and (30b) are plotted in Figure 24-27 with various values of L_f^* (from 1 to 10) and S_{min}^* < 10 or S_{min}^* > 10 (from 0.025 to 1000), respectively. The main purpose in this application is to test the solutions with changing the variables from very low values to high values, and observing how much those variables influence the results for different solutions. However, there is no significant deviation in the results for the considered values of L_f^* and S_{min}^*. Thus, any form of the proposed equations can be used instead of the original models.

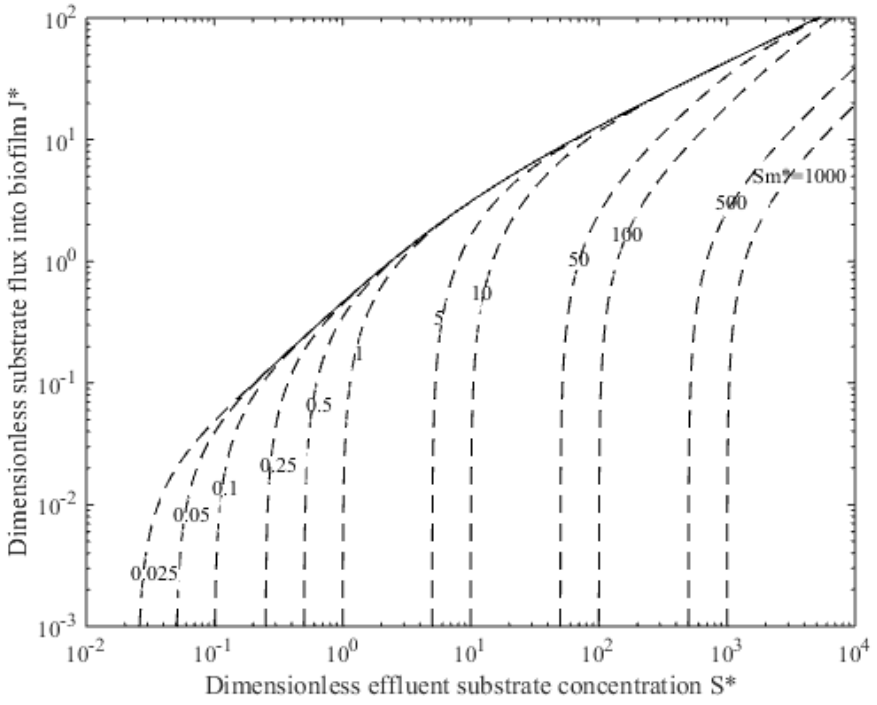

Figure 3- 19: Substrate flux *J** as a function of *S** and *Sm** when L_f =1(Eq31).

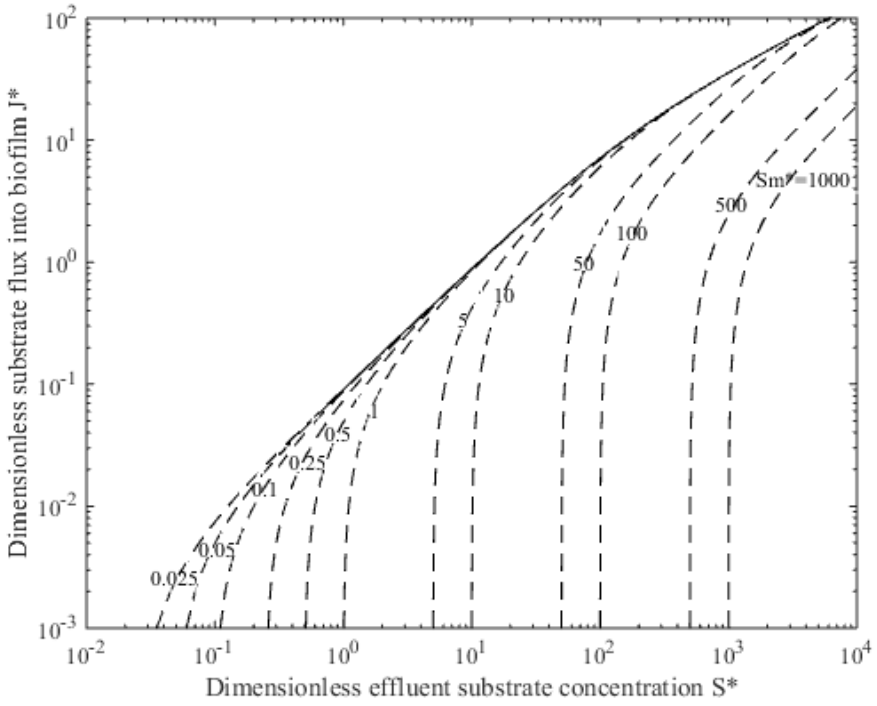

Figure 3- 20: Substrate flux J^* as a function of S^* and Sm^* when L_f=10 (Eq31).

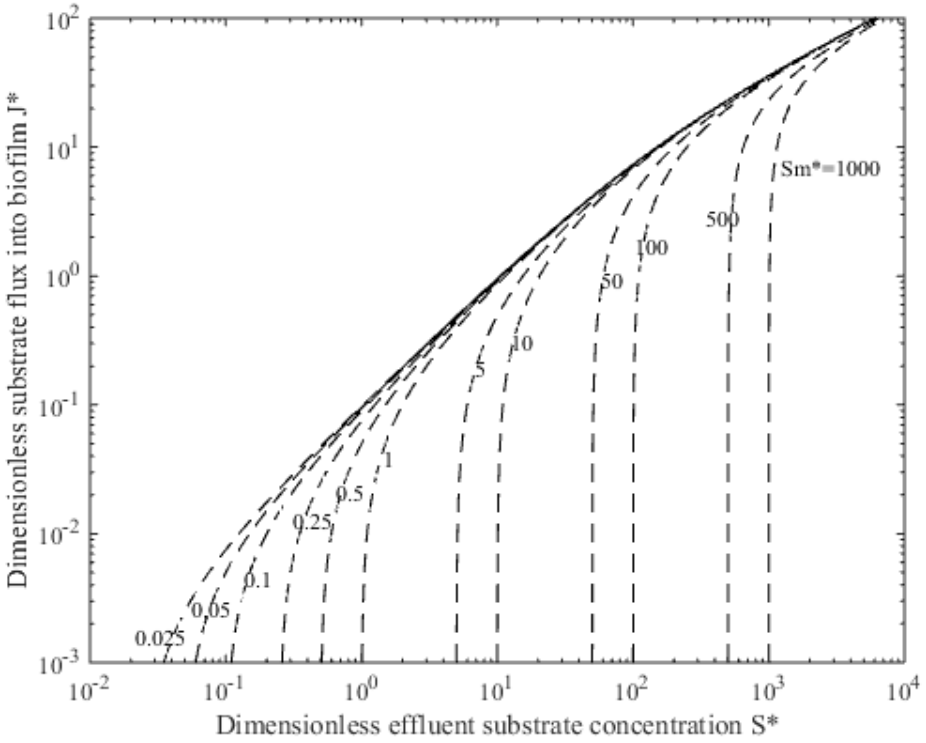

Figure 3- 21: Substrate flux J^* as a function of S^* and Sm^* when L_f =1 (Eq33).

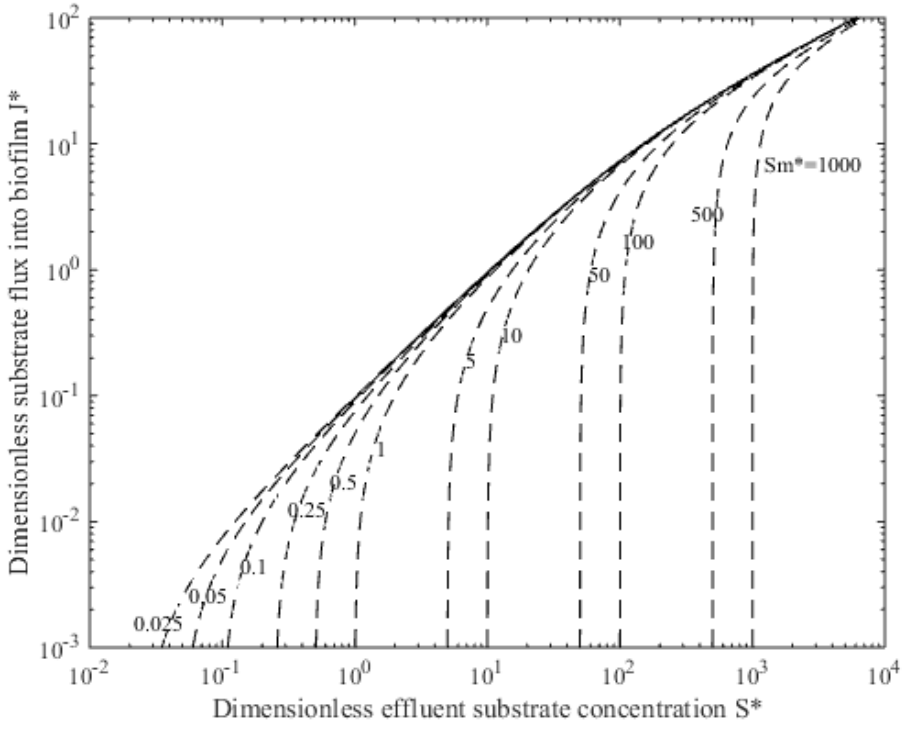

Figure 3- 22: Substrate flux J^* as a function of S^* and Sm* when L_f =10 (Eq33).

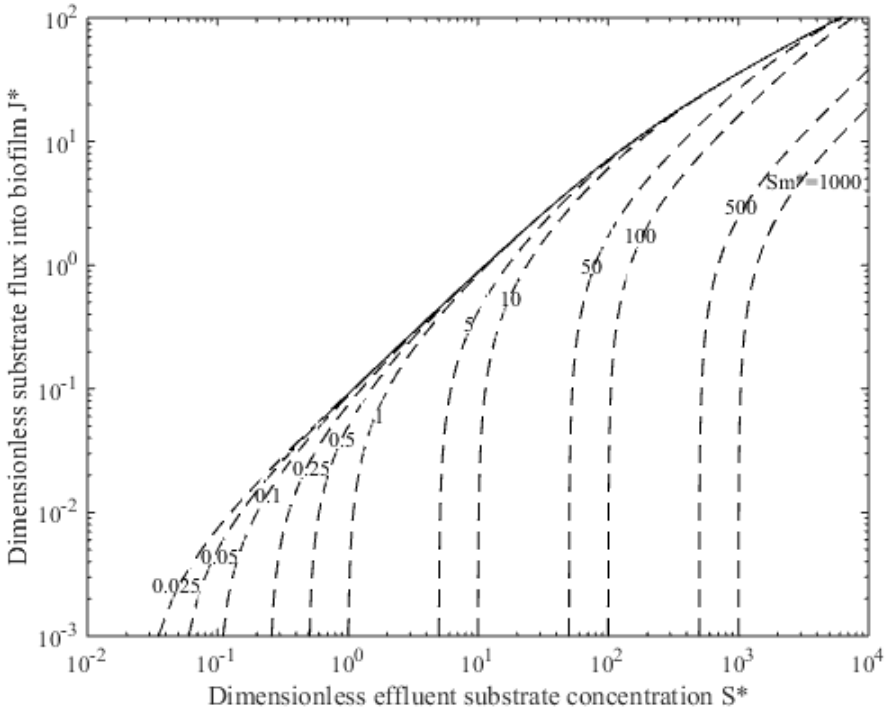

Figure 3- 23: Substrate flux J^* as a function of S^* and Sm^* when L_f =50 (Eq33).

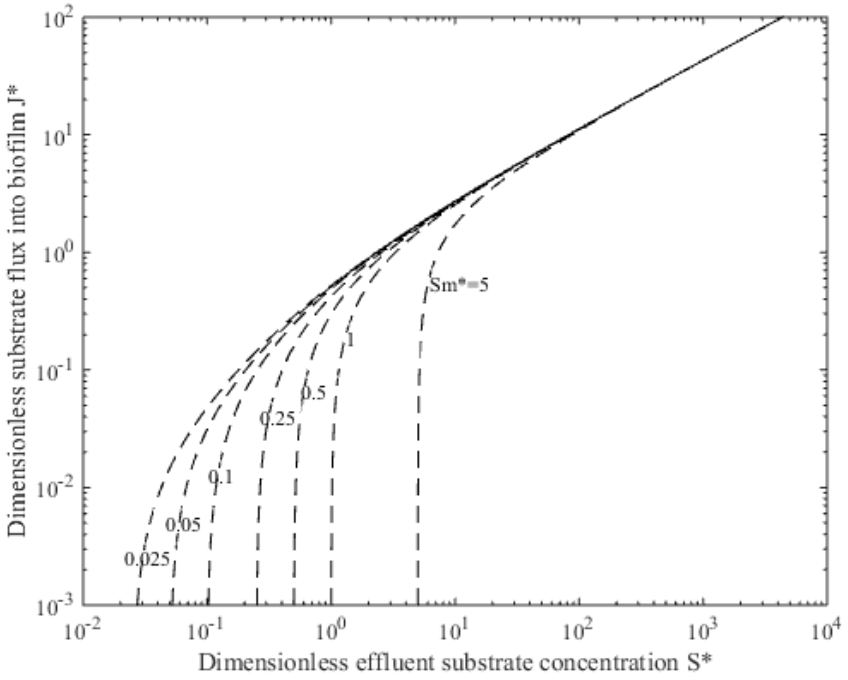

Figure 3- 24: Substrate flux J^* as a function of S^* and when Sm^* less than 10 and L_f =1 (Eq30a).

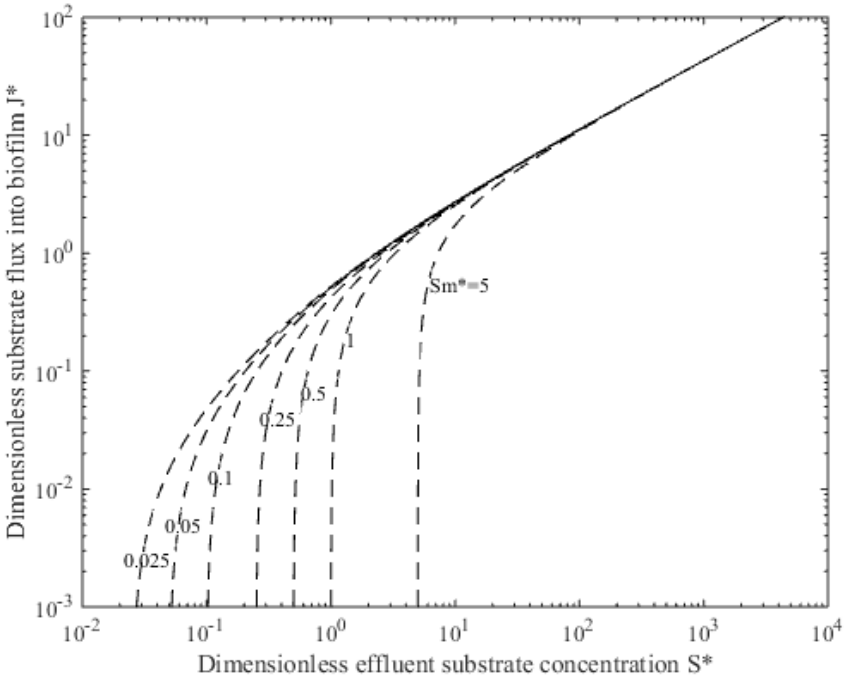

Figure 3- 25: Substrate flux J^* as a function of S^* and when Sm^* less than 10 and L_f =10 (Eq30a).

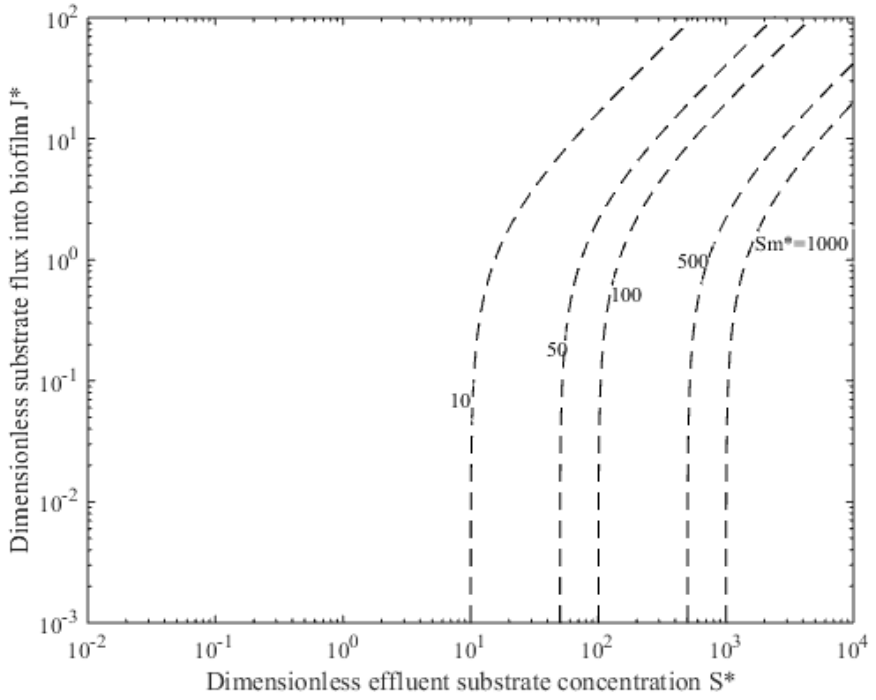

Figure 3- 26: Substrate flux J^* as a function of S^* and when $Sm^* > 10$ and $L_f = 1$ (Eq30b).

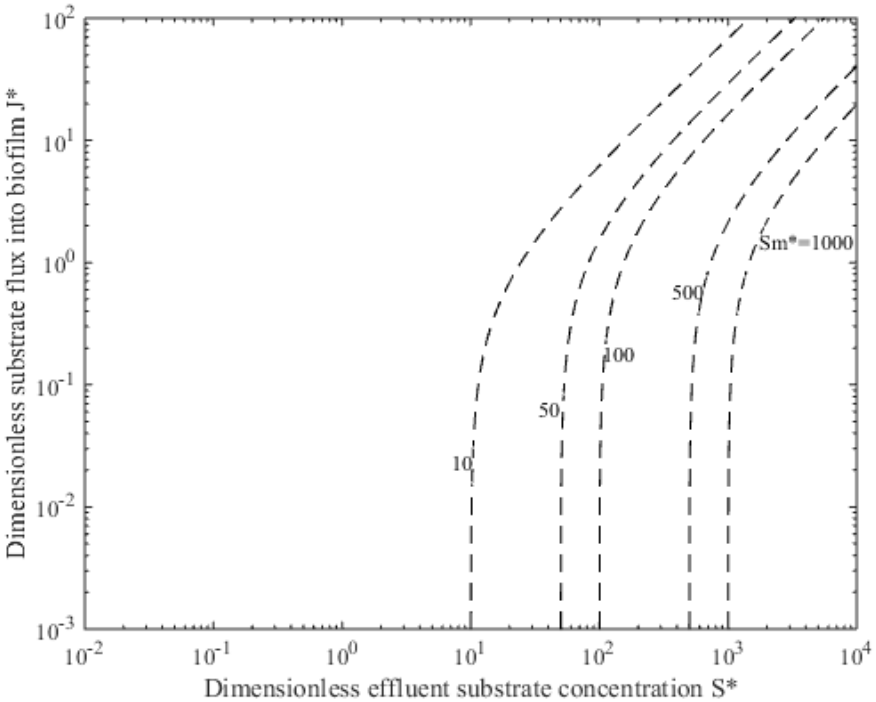

Figure 3- 27: Substrate flux J^* as a function of S^* and when $Sm^* > 10$ and $L_f = 10$ (Eq30b).

The following dimensionless equations and eq. 25 represent Fick's law, Monod expressions and mass balance of biofilm, which are the basic equations of the two models.

$$\frac{d^2 S_f^*}{dz^{*2}} = \frac{S_f^*}{1 + S_f^*} \quad (35)$$

$$\int_0^{L_f^*} \frac{S_f^*}{1 + S_f^*} dz^* = J^* \quad (36)$$

$$at\ z^* = 0, S_f^* = S_S^*\ and \frac{dS_f^*}{dz^*} = -J^* \quad (37)$$

$$at\ z^* = L_f^*, \frac{dS_f^*}{dz^*} = 0 \quad (38)$$

$$L_f^* = J^* \left(\frac{1}{S_{min}^*} + 1 \right) \quad (39)$$

where L_f^* is the dimensionless biofilm thickness, S_f^* is the dimensionless substrate concentration within biofilm, and z^* is the dimensionless distance normal to the biofilm thickness.

In order to test the different expressions, it will consider a specific wastewater having the characteristics and kinetic coefficients in Table 2-4 (Minkov et al., 2006). Also, given the influent substrate concentration S^o = 430.0 mg/L, and effluent substrate concentration S=5.0 mg/L, then S_{min} = $K_s/(YKm/b_t - 1)$=1.0 mg/L.

(a) Evaluation of J using eq. 34 (Saez and Rittmann proposed expression)

$$J = \left[\left(0.0078 \times 10 \times 25 \times \frac{0.75}{1.25} \right)^2 + 2 \times 10 \times 25 \times 0.75 \frac{5.0 - 1.0}{1000} \right]^{0.5} - 0.0078 \times 10 \times 25 \times \frac{0.75}{1.25}$$

$J = 0.52 mg cm^{-2} d^{-1}$

(b) Evaluation of J using the Saez and Rittmann model (1988) Various dimensionless parameters are computed as

$$S^* = \frac{5}{10} = 0.5, S^*_{min} = \frac{1.0}{10} = 0.1,$$

$$L^*_f = 0.0078[\frac{10 \times 25}{0.01 \times 0.75}]^{0.5} \times \frac{0.75}{1.25} = 0.85.$$

Simultaneous solution of the six equations comprising the model (eqs. 14-17) yields the following: α=1.69, β=0.52, f=0.91, J^*_{deep} =0.43, S^*_s=0.17, and J^*=0.39 from which J=0.53 $mg cm^{-2} d^{-1}$.

As shown above, the results from method (a) and (b) have similar values, and the first method is calculated using equation 34. Thus, this proposed expression for substrate flux into biofilm is used to test the experimental data and the biofilm kinetic parameters are selected in Table 2-3.

The modified equation represents the exact solution of the biofilm model and could be expressed in dimensional form. The simplicity and short structure of the modified equation allows easy simulation of biofilm. Additionally, it may be a useful tool to estimate the biofilm kinetics. Finally, the model can be used to design a biofilm reactor under different conditions for various parameters.

3.3.1 Experimental Data Discussion on Substrate Flux into Biofilm

Based on the solutions for testing the hypothetical data in the above equations, Equation 34 is used to simulate the experimental data for ultimate BOD in the modified model of substrate flux into biofilm. Figure 3-28 and 3-30 show effective biomass concentration *(L_i-L_o)* in which L_i and L_o represent the ultimate BOD concentration from

the inlet and outlet respectively, and both of them are calculated by different experimental data (BOD_5) selected from different seasons. Figure 3-29 describes the results of effective biomass concentration, and comparing the power curve which is plotted by a typical range of effective substrate concentrations from 0 to 0.015 mg/cm^3. Figure 3-31 gives the relationship between biomass concentration and effective substrate concentration. It is clear to see the values of flux stay at similar levels in each season. In other words, the biological processes are totally different in the various seasons. However, due to the limitation of the experimental input data, we cannot determine if there is a significant effect on the results of substrate flux into biofilm because of the small number of experimental data used and the fixed the biofilm parameters such as biofilm thickness in the model.

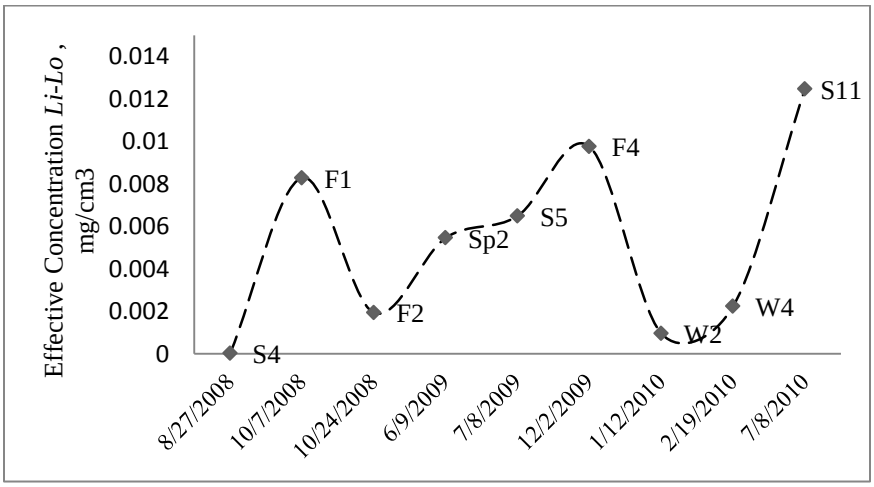

Figure 3- 28: Selected experimental data for effective substrate concentration L_i-L_o (ultimate BOD).

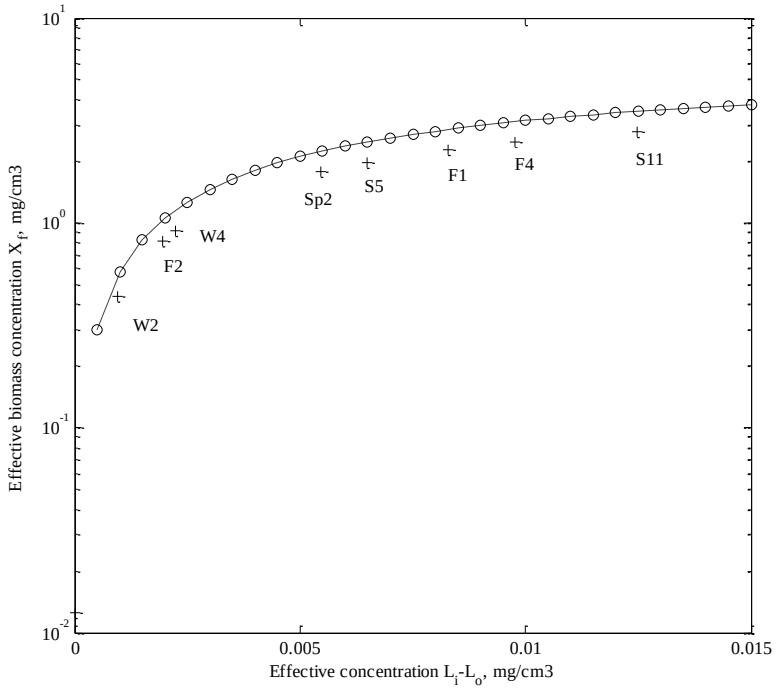

Figure 3- 29: Effective biomass concentration X_f was computed by selected experimental data (ultimate BOD).

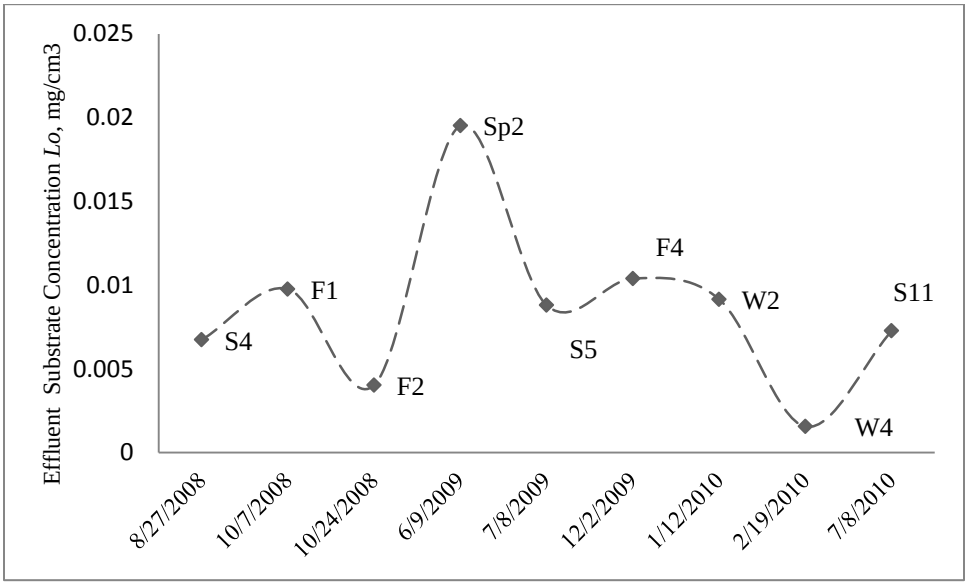

Figure 3- 30: Selected experimental data for effluent substrate concentration L_o (ultimate BOD).

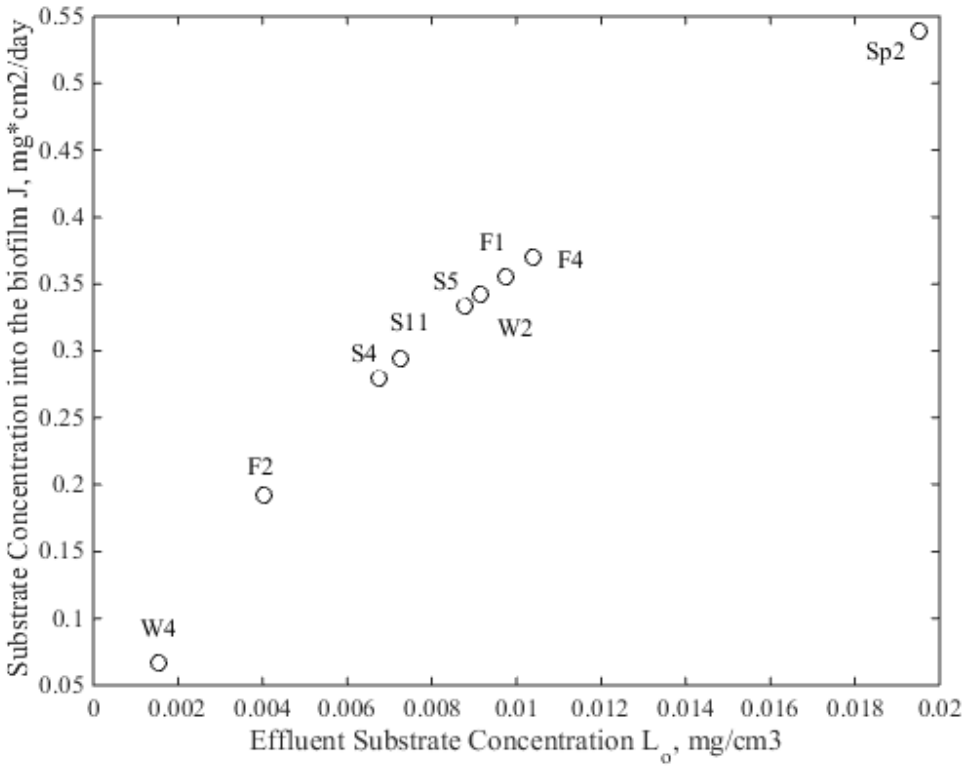

Figure 3- 31: Substrate flux *J* as a function of effluent substrate concentration L_o computed by selected experimental data (ultimate BOD)

3.4 Computer models of biofilm growth

The following figures show a monospecies 2D biofilm model program developed by a biofilm modelling group at TU Delft. By changing the microorganism and environment properties, and testing the program around the 30 day mark, the program will illustrate the results with different shapes of biofilm formation. Also, a single species biofilm with a single solute species (oxygen) is considered in this model, and the growth rate and oxygen consumption rate are presented in this research.

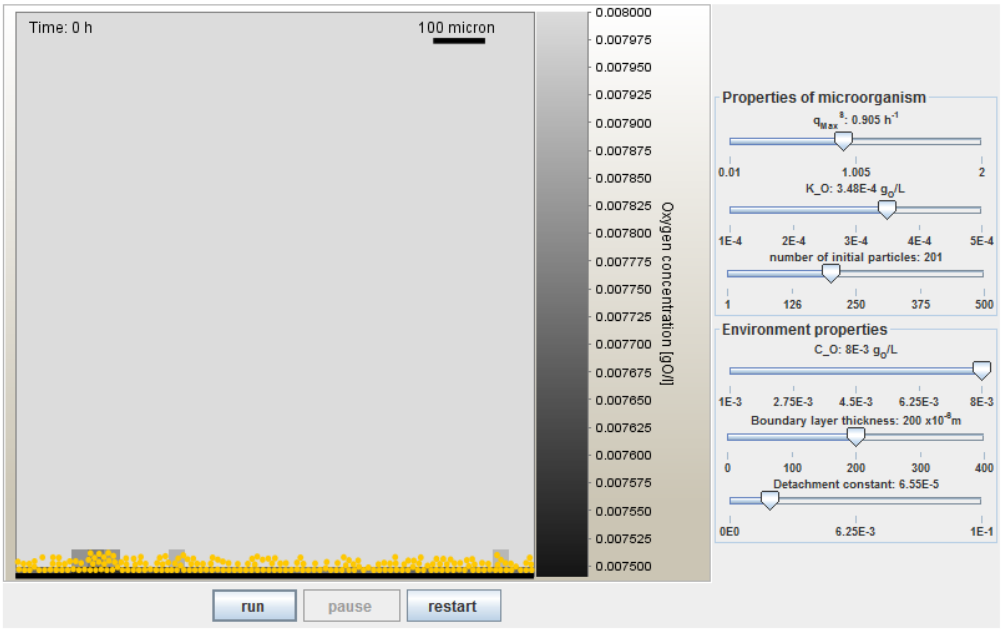

Figure 3- 32: a monospecies 2D biofilm model (2004, Biofilm modelling group at the TU Delft)

The software is used as a demonstration of the framework for biofilm modeling. As the figure shows, you can change both microorganism and environment properties for the modeling by moving the property sliders. In addition, this model illustrates a single species biofilm with a single solute species (oxygen) being considered. In order to allow their simulations to reach a steady state when growth is balanced by detachment, biomass detachment must also be considered in this model. Moreover, the following equations describe the definition for model kinetics.

Biomass growth rate:

$$r_x = qY\frac{S}{S+K_m}X_f \qquad (40)$$

Oxygen consumption rate:

$$r_o = -q(1-Y)\frac{S_{bo}}{(S_{bo}+K_m)}X_f \qquad (41)$$

Detachment equation:

$$r_{det} = k_{det} X^2 X_f \qquad (42)$$

where q is the maximum specific substrate uptake rate of the microorganism, K_m is oxygen half saturation constant, k_{det} is the detachment rate constant, X is the distance to the solid surface, X_f is biomass concentration and S_{bo} is bulk liquid concentration of oxygen. It is noted that the value used for the yield of biomass on substrate Y is 0.495 which is not controlled by sliders in the program.

Before running the program, you need to set up the model parameters by moving the sliders. The following are the meanings of each parameter in this model:

- q^s_{max} - The maximum specific substrate uptake rate of the microorganism
- *K_O* - Oxygen half saturation constant of microorganism
- Number of initial particles - Number of particles for inoculation of the system
- *C_O* - Bulk liquid concentration of oxygen
- Boundary layer thickness - The thickness of the concentration boundary layer.
- Detachment constant (k_{det}) - The detachment rate constant.

It is noted that decreasing the thickness will decrease the effect of diffusion limitation of oxygen on the biofilm. However, when you change the detachment constant slider, then detachment will increase with the square of the distance to the solid surface. Based on the instruction of this program, we run two experiments with different situations to produce some biofilm modelling simulations.

3.4.1 Roughness development in unstressed biofilms

In the previous research, biofilm studies have shown that roughness of biofilms growing in the absence of detachment forces depends on the mass transport regime of a

growth limiting solute. Biofilms grown will develop a flat morphology while diffusion limitation of the growth limiting solute is not significant. In contrast, biofilms will develop a finger like structure while diffusion limitation is significant. The user can run the model with two different conditions: smooth biofilm and rough biofilm, to produce results for a biofilm grown in oxygen limited conditions. The user needs to turn off detachment completely in these two cases (1) and (2) below, which means you have to set the detachment value to 0.

(1) Set up the model parameters for a smooth biofilm test, then press 'run' button:

- set up the detachment to zero
- Set up the boundary layer thickness to 0
- Set up high value for the oxygen concentration S to 8×10^{-3} g/L
- Set up q=0.01 per hour and 201 for initial particles

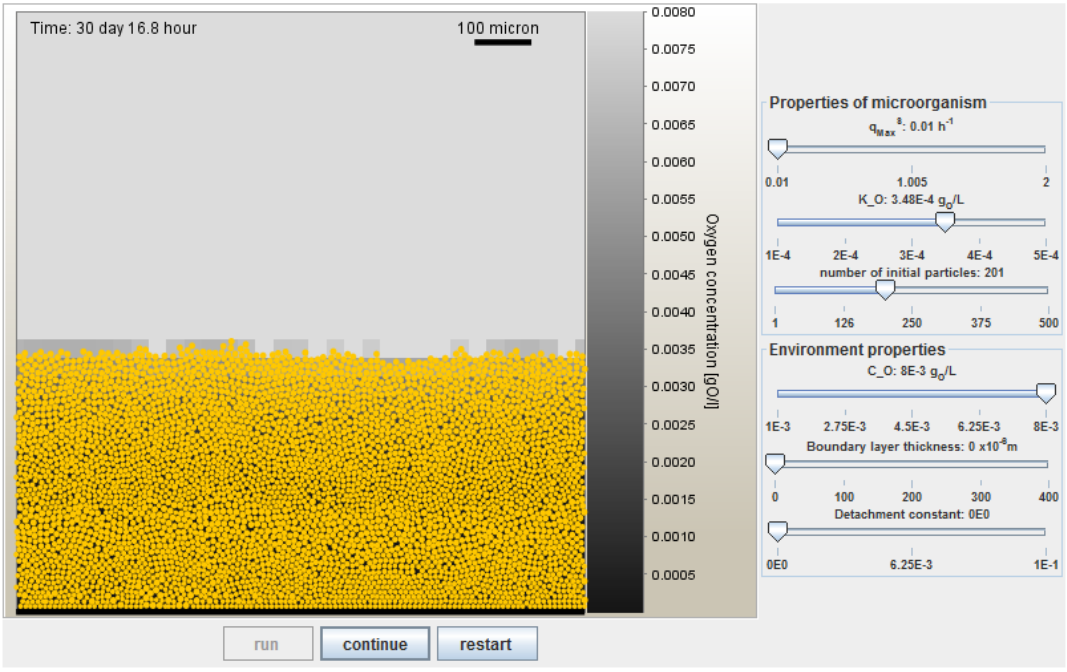

Figure 3- 33: Smooth Biofilm Formation

After around 30 days shown in the screen you should stop the program and observe the morphology of the biofilm which is smooth. In addition, when the number of biomass particles in the simulation becomes large, the spreading step becomes the limiting step of the simulation. In this case, at about day 30 the simulation will become significantly slower.

(2) Set up the model parameters for rough biofilm test, then press ‘run’ button:

- Set up the detachment to zero
- Set up the boundary layer thickness to 256×10^{-8}m
- Set up low value for the oxygen concentration S to 1×10^{-3} g/L
- Set up q=1.343 per hour and 201 for initial particles

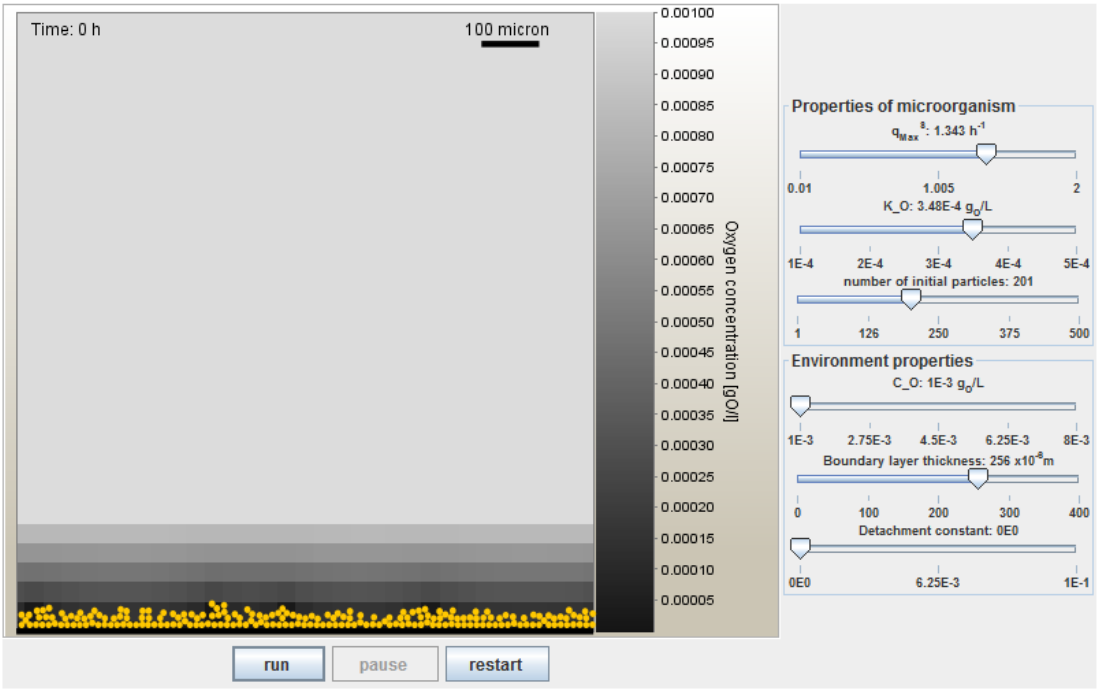

Figure 3- 34: Rough Biofilm Testing Setup

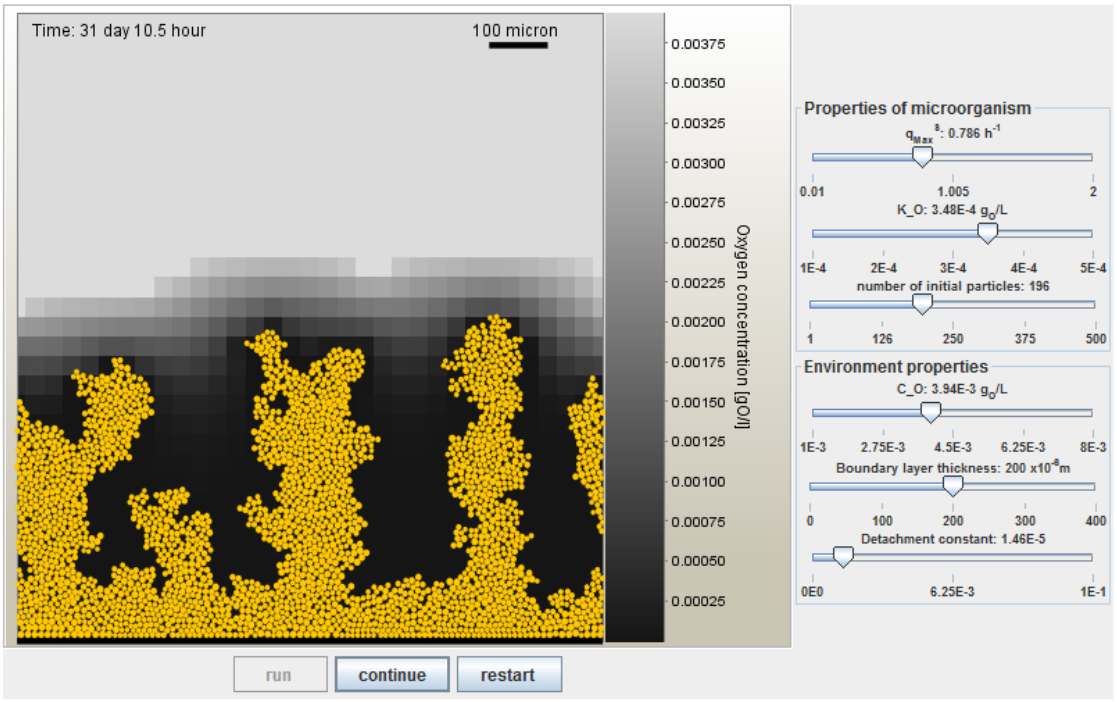

Figure 3- 35: The shape of Rough Biofilm Formation

This roughness of the biofilm will be more pronounced the higher you set the values of the boundary layer thickness and *q*.

3.4.2 Steady state of biofilm under oxygen limitation

In this part, a steady state biofilm under one substrate limitation is considered. For biofilms grown under the same conditions, applying increased detachment forces may induce the occurrence of sloughing events and the formation of a smooth biofilm. In this test we will illustrate how to create a biofilm showing a rough morphology and in steady state where sloughing events will present. After that, detachment forces will increase to lead to a morphology change to a smooth biofilm, removing the occurrence of sloughing events.

(3) Set up the model parameters for steady state rough biofilm test under oxygen limitation, then press 'run' button:

- Set up the detachment to 8×10^{-4}
- Set up the boundary layer thickness to 400×10^{-6}m
- Set up low value for the oxygen concentration S to 8×10^{-3} g/L
- Set up q=2 per hour and 121 for initial particles

At about day 31 the first sloughing event will occur. After that, the biofilm structure shows a steady state, in which tall group will rise and reduce in a cyclic fashion.

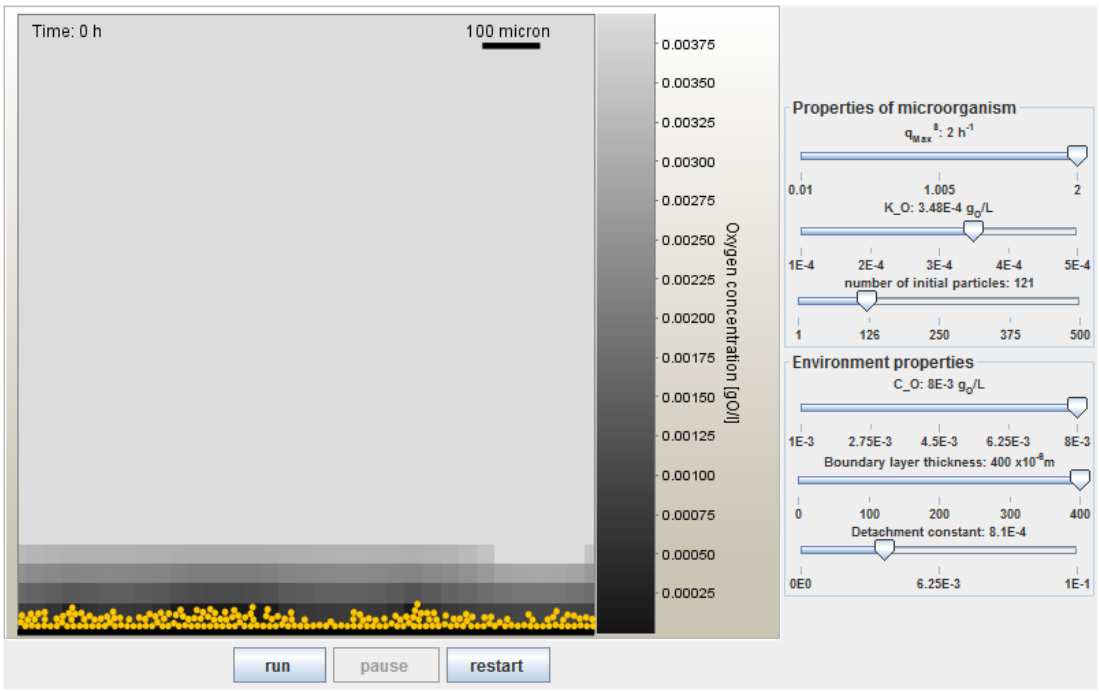

Figure 3- 36: Steady state of biofilm under oxygen limitation Testing Setup

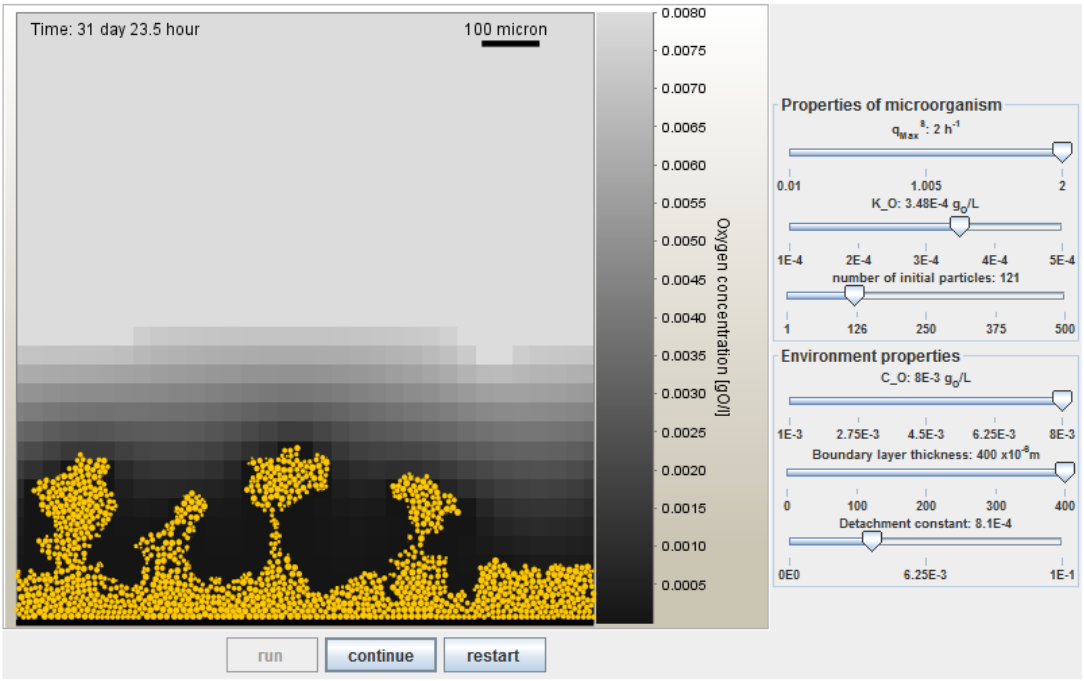

Figure 3- 37: The shape of biofilm formation under oxygen limitation

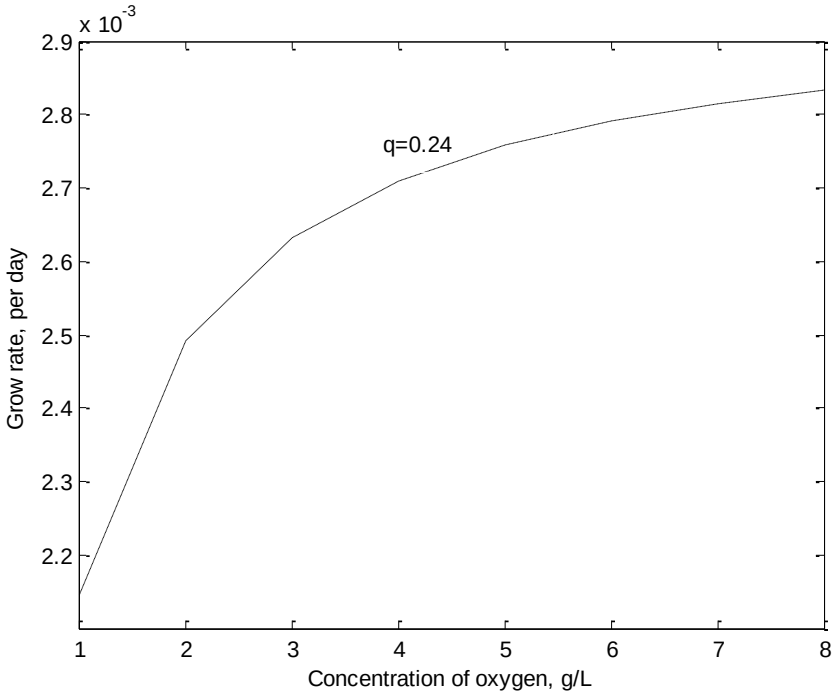

Figure 3- 38: The biomass growth rate was computed with various values of oxygen concentration

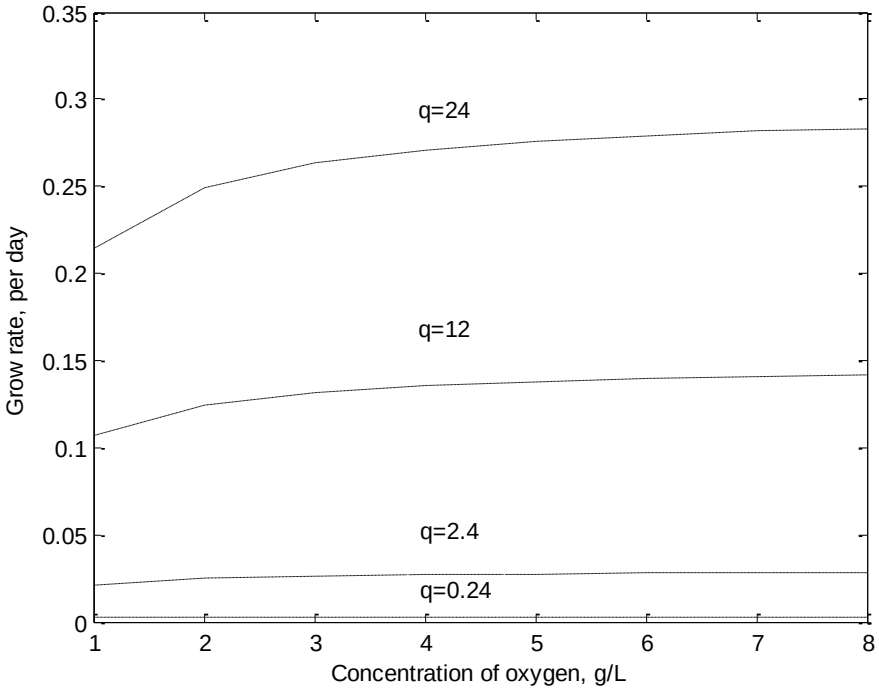

Figure 3- 39: The biomass growth rate was computed with various values of *q*

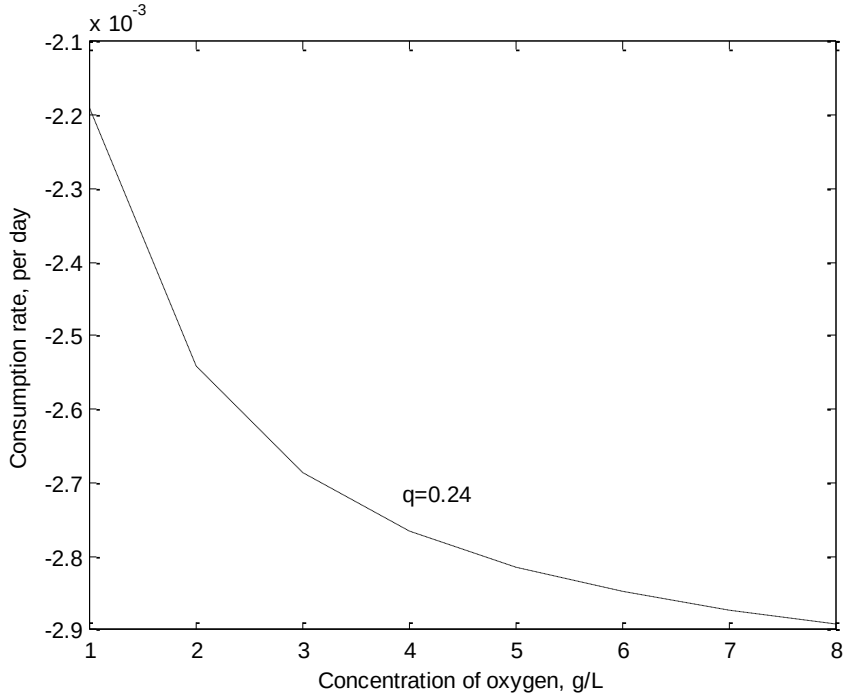

Figure 3- 40: The oxygen consumption rate was computed with various values of oxygen concentration

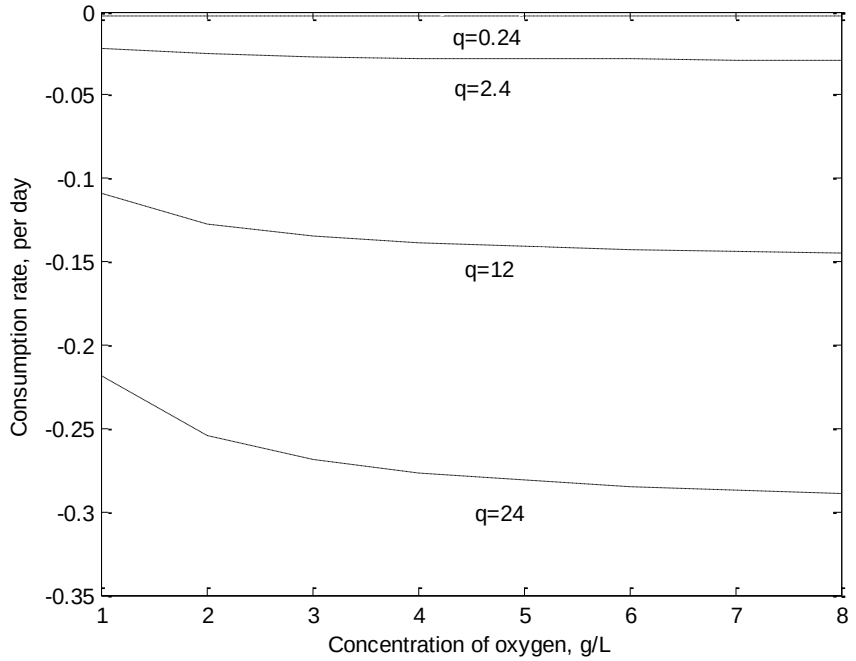

Figure 3- 41: The oxygen consumption rate was computed with various values of *q*

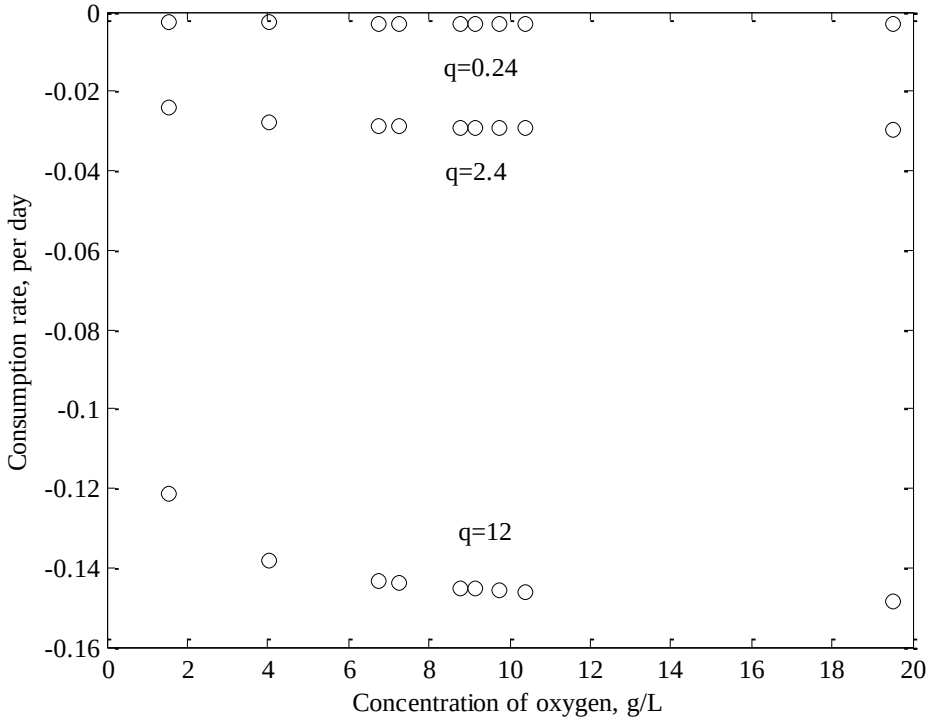

Figure 3- 42: The oxygen consumption rate was computed with various values of *q* by experimental data (ultimate BOD)

Equation 40 and 41 give the introduction of expressions that define kinetics for the model. They are biomass growth and oxygen consumption rate respectively, and recall the equation 11 in chapter 2 that describes microbial growth with decay within the biofilm (Ghannoum et. al, 2004), in which growth is represented by a Monod-type expression (first term on right-hand side of equation 11). In this model, the biomass growth rate and oxygen consumption rate are influenced by the biofilm kinetic parameters such as the concentration of oxygen in the bulk liquid. It is easy to move the sliders by changing microorganism and environment properties in this model, however, how do those parameters affect the results are still considered mathematical. Figure 3-38 illustrates the biomass growth rate increases while the concentration of oxygen goes up. Moreover, figure 3-39 offers the maximum specific substrate uptake rate of microorganism has significantly large effect on the growth rate, and its growth will lead to a high value of the biomass growth rate. Finally, figure 3-40 and 3-41 show that oxygen consumption is expected to be a negative value and its value will decrease while increasing the maximum specific substrate uptake rate of microorganism. Finally, figure 3-42 was plotted with experimental data (BOD), and the results show that the range of consumption rate is similar with the rate in figure 3-41 which is computed with the same values of q.

Chapter 4: Conclusions and Future Work

4.1 Conclusions and Discussion

This research focused on modeling the biofilm activity in a bioretention cell by running mathematical models of biofilm with experimental data. A mathematical model describing the nitrification and BOD processes combined in a single biofilm was developed. The sensitivity of various parameters to the process performance was analyzed. With a sensitivity analysis, the solutions of the mathematical model of substrate and biomass concentration into biofilm were tested by using both hypothetical data and experimental data, and the results showed that the substrate concentration inside the biofilm will be extremely influenced by substrate concentration outside the biofilm and biofilm thickness, while effective biomass concentration will increase when the effective substrate concentration grows. In addition, the value of effective biomass concentration was supposed to be positive which implies biofilm activity uptake in that period. Based on the experimental data for NO_3^-, the results showed the biological processes mostly occur in the summer term, this may be due to various factors such as temperature, climate and plant growth in that season. On the other hand, the results of the value of substrate flux into biofilm went up when the substrate concentration increased, moreover, the experimental data for ultimate BOD was simulated in the modified model of substrate flux into biofilm by Equation 34 which showed the value of flux stayed at the same level in each season. In this case, the biological processes worked by different compounds in the mathematical model to gave various biological or bioremendiation results, particularly for nitrogen compounds because bioretention cells are not very effective in reducing the concentration of nitrate - this is due to the fact that nitrate is more stable

than other compounds in the cells. However, the various inputs by experimental data did not have too much influence on the results of substrate concentration, biomass concentration and substrate flux into biofilm. This is because we used typical kinetic parameters from the previous model studies, and we fixed the biofilm parameters such as biofilm thickness. Generally, the substrate concentration outside the biofilm changed within a typical range from 0.0005 to 0.05 mg/cm^3 which could lead to the change for other parameters such as biofilm thickness, but normally you would like to fix this value because such parameters are hard to measure and uncontrolled.

4.2 Future Work

There is plenty of work that should be further conducted related to the research in this thesis. As mentioned before, vegetation may be the most important component for nitrogen removal in bioretention cells. Providing suggestions for how to structure a macro-scale model of bioretention cell's bioremediation processes should be a main objective of future work.

The design and operation of biofilm reactors for improved nutrient removal of stormwater in bioretention cells is ultimately dependent on our ability to gain a clearer understanding of both bulk-phase and biofilm processes. In the future, if the objective is to focus on describing the performance of a biofilm system at the macroscale, then there are various compartments and processes that do not necessarily need to be described in too much detail, while considering the initial conditions at the microscale. A lot of detail at the microscale makes the model more difficult to create and compute. For instance, if the biofilm is quite deep, then the biofilm thickness is not a model feature of importance when substrate flux is the research objective, because thickness does not greatly influence

the flux for a deep biofilm. In contrast, if the objective is to model micro-scale processes, then more micro-scale parameter details need to be presented in the model, and more complex processes are needed such as 2d or 3d model with μm-scale. Macro-scale outputs in biofilm models include substrate removal rates, biomass accumulation and biomass loss from the system. In this case, substrate removal in the bioretention cells is the main concern in future research and particularly in the design and characterization of biofilm reactors.

In this research, biofilm kinetics parameters are used from previous studies, and most of them are from wastewater. It is known that those parameters from wastewater are totally different that the corresponding values for stormwater. Stormwater is water from other sources that drains into a street drainage system, thus, the influent and effluent substrate concentration is uncontrolled and is not constant. More importantly, the biofilm kinetic parameters are hard to measure and monitor, and nutrient levels also vary. In this case, there is no literature on values for stormwater to the author's knowledge. The Equation 4 in this research is the model for mass balances for substrate in the bulk liquid, and the substrate can be any soluble component such as organic substrate, BOD, COD O_2, NH_3, etc. The equation illustrates the difference between the substrate in the influent and effluent transferred through the biofilm system. In our bioretention cell, we have no idea how much specific surface area is on the root surface but we also need the average substrate flow rate in the system, so this is a good direction for further research which focuses on the surface area for biofilm formation in bioretention cells. Bioretention cells are a good start to focus on stormwater, which could store the stormwater, analyze

nutrient reduction and other properties in a real site. Thus, some monitoring devices for biofilm parameters are required for future research in the field work.

REFERENCE

Ancion, Pierre-Yves, et al. "Using biofilm as a novel approach to assess stormwater treatment efficacy." *Water research* 49 (2014): 406-415.

Barbosa, A. E., J. N. Fernandes, and L. M. David. "Key issues for sustainable urban stormwater management." *Water research* 46.20 (2012): 6787-6798.

Beattie, Gwyn A. "Plant-associated bacteria: survey, molecular phylogeny, genomics and recent advances." *Plant-associated bacteria*. Springer Netherlands, 2006. 1-56.

Biazar, J., and R. Islam. "Solution of wave equation by Adomian decomposition method and the restrictions of the method." *Applied Mathematics and Computation* 149.3 (2004): 807-814.

Compant, Stéphane, Christophe Clément, and Angela Sessitsch. "Plant growth-promoting bacteria in the rhizo-and endosphere of plants: their role, colonization, mechanisms involved and prospects for utilization." *Soil Biology and Biochemistry* 42.5 (2010): 669-678.

Costerton, J. William, et al. "Microbial biofilms." Annual Reviews in Microbiology 49.1 (1995): 711-745.

Danhorn, Thomas, and Clay Fuqua. "Biofilm formation by plant-associated bacteria." Annu. Rev. Microbiol. 61 (2007): 401-422.

Donlan, Rodney M. "Biofilms: microbial life on surfaces." Emerg Infect Dis 8.9 (2002).

Eberl, Hermann. *Mathematical modeling of biofilms*. Vol. 18. IWA publishing, 2006.

Fouad, Moharram, and Renu Bhargava. "Modified expressions for substrate flux into biofilm." Journal of Environmental Engineering and Science 4.6 (2005): 441-449.

Fouad, Moharram, and Renu Bhargava. "A simplified model for the steady-state biofilm-activated sludge reactor." *Journal of environmental management* 74.3 (2005): 245-253.

Fuqua, Clay, and Ann G. Matthysse. "Methods for studying bacterial biofilms associated with plants." Methods in enzymology 337 (2001): 3.

Ghannoum, Mahmoud, and George A. O'Toole. *Microbial biofilms*. ASM Press, 2004.

Ghodsalavi, Behnoushsadat, et al. "Isolation and characterization of rhizobacteria and their effects on root extracts of Valeriana officinalis." (2013): 338.

Goudar, Chetan T., and Keith A. Strevett. "Computer programs for estimating substrate flux into steady-state biofilms from pseudoanalytical solutions."Computer Applications in Engineering Education 10.1 (2002): 26-32.

Jaradat, Omar K. "Adominn Decomposition Method for Solving A belimi Differential Equations." *Journal of Applied Sciences* 8.10 (2008): 1962-1966.

Khan, Usman Taqdees, et al. "Bioretention cell efficacy in cold climates."*Masters Abstracts International*. Vol. 50. No. 01. 2011.

Lakshmanan, Venkatachalam, Amutha Sampath Kumar, and Harsh P. Bais. "The ecological significance of plant-associated biofilms." *Microbial biofilms: Current research and applications. Caister Academic Press, Norfolk* (2012): 43-60.

Lear, Gavin, and Gillian D. Lewis, eds. *Microbial biofilms: current research and applications*. Horizon Scientific Press, 2012.

Makinde, O. D. "Adomian decomposition approach to a SIR epidemic model with constant vaccination strategy." *applied Mathematics and Computation*184.2 (2007): 842-848.

McNear Jr., D. H. The Rhizosphere - Roots, Soil and Everything In Between. *Nature Education Knowledge* (2013) 4(3):1.

Meima, J. A., N. Mora Naranjo, and A. Haarstrick. "Sensitivity analysis and literature review of parameters controlling local biodegradation processes in municipal solid waste landfills." *Waste management* 28.5 (2008): 904-918.

Min'kov, L. L., S. V. Pyl'nik, and J. H. Dueck. "Steady-state problem of substrate consumption in a biofilm for a square law of microbial death rate." Theoretical Foundations of Chemical Engineering 40.5 (2006): 496-502.

Mohamed, M. A. "Comparison differential transformation technique with Adomian decomposition method for dispersive long-wave equations in (2+ 1)-dimensions." *Applications and Applied Mathematics* 5.1 (2010): 148-166.

Muthukaruppan, Subramanian, Alagu Eswari, and Lakshmanan Rajendran. "Mathematical modelling of a biofilm: The Adomian decomposition method."Natural Science 5.04 (2013): 456.

Noguera, Daniel R., Gonzalo E. Pizarro, and John M. Regan. "Modeling biofilms." *Microbial biofilms* (2004): 222-250.

O'Toole, George, Heidi B. Kaplan, and Roberto Kolter. "Biofilm formation as microbial development." Annual Reviews in Microbiology 54.1 (2000): 49-79.

O'Toole, George A., and Mahmoud A. Ghannoum. "Introduction to Biofilms: Conceptual Themes." (2004): 1-3

Pastorella, Gabriele, et al. "Biofilms: applications in bioremediation."*Microbial Biofilms-Current Research and Applications* (2012): 73-98.

Prpich, George P., and Andrew J. Daugulis. "Biodegradation of a phenolic mixture in a solid–liquid two-phase partitioning bioreactor." *Applied microbiology and biotechnology* 72.3 (2006): 607-615.

Ramey, Bronwyn E., et al. "Biofilm formation in plant–microbe associations."Current opinion in microbiology 7.6 (2004): 602-609.

Rittmann B. 2004. Biofilms in the Water Industry, p 359-378. *In* Ghannoum M, O'Toole G (ed),*Microbial Biofilms*. ASM Press, Washington, DC. doi: 10.1128/9781555817718.ch19

Rudrappa, Thimmaraju, Meredith L. Biedrzycki, and Harsh P. Bais. "Causes and consequences of plant-associated biofilms." FEMS microbiology ecology64.2 (2008): 153-166.

Sáez, Pablo B., and Bruce E. Rittmann. "Error analysis of limiting-case solutions to the steady-state-biofilm model." *Water Research* 24.10 (1990): 1181-1185.

Siddiqui, A. M., et al. "Use of Adomian decomposition method in the study of parallel plate flow of a third grade fluid." *Communications in Nonlinear Science and Numerical Simulation* 15.9 (2010): 2388-2399.

Stoodley, P., and P. Dirckx. "Biofilm formation in 3 steps." (2003).